Modulation of Neurovascular Coupling in the Retina:

Effects of Oxygen and Diabetic Retinopathy

A DISSERTATION SUBMITTED TO THE FACULTY OF THE GRADUATE SCHOOL OF

THE UNIVERSITY OF MINNESOTA

By

Anusha Mishra

IN PARTIAL FULFILLMENT OF THE REQUIREMENTS FOR THE DEGREE OF

DOCTOR OF PHILOSOPHY

Advisor: Eric A. Newman

June, 2011

Acknowledgements

I thank my advisor Eric Newman for welcoming me into the lab, for teaching me everything I know about retinal work, for being patient with me when I could not remember how to do things, and, above all, for training me to be a critical scientist.

I thank my committee chair Paulo Kofuji for being supportive and always being available to bounce ideas off of.

I thank Michael Burian for his expert technical assistance and sensible advice.

I thank Monica Metea, Ben Clark and Zeb Kurth-Nelson for helping me with techniques in the lab when I first started.

I thank the current lab members, Anja Srienc, Tess Kornfield and Joanna Kur, for many wonderful, passionate discussions, both scientific and personal.

I thank Arif Hamid for his excitement for science, and for helping me with so many experiments.

I thank Steve Sullivan for always being there to brainstorm ideas with, for reading all my initial drafts, for moral support and for always pushing me to think big.

I thank my committee members, Cheryl Olman and Esam El-Fakahany, for their support and encouragement throughout this process.

I dedicate this thesis to my Dad, who made sure I would have an education despite all obstacles,

and my Mom, who encouraged me to go explore the world when I was too scared to do so.

Abstract

Neurovascular coupling is a process by which neuronal activity leads to localized increases in blood flow in the central nervous system. When neurovascular coupling results in hyperperfusion of the neural tissue, the response is termed functional hyperemia and serves to satisfy the increased energy demand of active neurons. In brain slices, high [O_2] alters neurovascular coupling, decreasing activity-dependent vasodilations and increasing vasoconstrictions. However, *in vivo*, hyperoxia has no effect on neurovascular coupling. In order to resolve these conflicting reports of O_2 modulation, I examined neurovascular coupling in both *ex vivo* and *in vivo* rat retina preparations. In the *ex vivo* retina, 100% O_2 reduced the amplitude of light-evoked arteriole vasodilations by 3.9-fold and increased the amplitude of vasoconstrictions by 2.6-fold when compared to responses in atmospheric [O_2] (21%), consistent with slice data. Oxygen exerted its effect by decreasing vasodilatory prostaglandin signaling and increasing vasoconstrictory 20-hydroxyeicosatetraenoic acid signaling. However, *in vivo*, hyperoxia (breathing 100% O_2) had no effect on light-evoked arteriole vasodilations or on blood flow. We found that the differing effects of O_2 arise because retinal pO_2 increases to a much greater extent in the *ex vivo* preparation (to 548 mmHg) than *in vivo* (to 53 mmHg; Yu et al. Am J Physiol 267:H2498-H2507). When retinal pO_2 was raised to 53 mmHg in the *ex vivo* retina, no change in neurovascular coupling was observed. These results demonstrate that although O_2 can modulate neurovascular signaling pathways when pO_2 is raised high enough, such levels are not attained *in vivo*, even when an animal breaths 100% O_2.

Functional hyperemia can also be modulated by pathological conditions. It is diminished in the retinas of diabetic patients, possibly contributing to the development of diabetic retinopathy. I investigated the mechanism responsible for this loss in a streptozotocin-

induced rat model of type 1 diabetes. Here I show that light-evoked arteriole dilation was reduced by 58% in these diabetic rats at 7 month survival time. The diabetic retinas showed neither a decrease in the thickness of the retinal layers nor an increase in neuronal loss, although signs of early glial reactivity were observed. Functional hyperemia is believed to be mediated, at least in part, by glial cells and we found that glial-evoked vasodilation was reduced by 60% in diabetic animals. An upregulation of inducible nitric oxide synthase (iNOS) was detected by immunohistochemistry, and inhibition of iNOS restored both light- and glial-evoked dilations to control levels. These findings suggest that high NO levels resulting from iNOS upregulation alters glial control of vessel diameter and may underlie the loss of functional hyperemia observed in diabetic retinopathy.

I further tested whether inhibiting iNOS reverses the loss of flicker-induced vasodilation in diabetic rat retinas *in vivo*. Flicker-evoked arteriolar dilations were diminished by 61% in diabetic animals, compared to non-diabetic controls. Treating diabetic animals with aminoguanidine (an iNOS inhibitor), either acutely via IV injection or long-term in drinking water, restored flicker-induced arteriole dilations in diabetic rats to control levels. The amplitude of the electroretinogram b-wave was similar in control and diabetic animals, suggesting that the deficit in functional hyperemia was not due to a reduction in neuronal activity. These findings demonstrate that inhibiting iNOS with AG is effective in preventing the loss of, and restoring, normal flicker-induced vasodilation in the diabetic rat retina. Treatment with iNOS inhibitors early in the course of diabetes has the potential to slow the progression of retinopathy by maintaining normal neurovascular coupling.

TABLE OF CONTENTS

LIST OF TABLES

Chapter 2

LIST OF FIGURES

Chapter 1

Chapter 2

Chapter 2

Chapter 3

Chapter I: Introduction

The central nervous system has a very high energy demand, and is supplied by an extensive network of blood vessels to meet its needs. Although the brain only comprises 2% of body mass in humans, it accounts for almost 20% of the body's energy usage (1). It is essential that cerebral blood flow be tightly regulated to maintain the health and activity of neurons. This is accomplished via multiple mechanisms, including autoregulation and functional hyperemia (2-5).

Autoregulation is a process that is evident in many biological systems, whereby blood flow is adjusted to maintain a constant rate of blood flow, and thus oxygen supply, in the face of varying blood pressure. Autoregulatory control of cerebral perfusion is important as too little perfusion can result in ischemic injury, while too much perfusion can increase intracranial pressure (which also eventually leads to ischemic injury), both being undesirable conditions for optimal health of the brain (2;6). Cerebral autoregulation occurs primarily by adjustment of cerebrovascular resistance, but neurogenic factors also play an important role in maintaining constant cerebral perfusion (2). In addition, a metabolic autoregulatory pathway serves to tune cerebral blood flow in response to fluctuations in lactate, CO_2, O_2 etc (7;8). Cerebral autoregulation, and the processes that contribute to it, are well characterized and reviewed in (6;9-11).

Functional hyperemia, in contrast, is the process by which a local increase in neuronal activity induces a corresponding increase in regional blood flow. This increase in blood flow occurs with high temporal and spatial fidelity. Neurovascular coupling occurs throughout the nervous system, including the retina, and serves to satisfy the increased

energy demand of active neurons. Our understanding of the mechanisms underlying functional hyperemia is still incomplete and many important questions have yet to be resolved (5).

Functional hyperemia was first described by Mosso in 1880 (12). It was further characterized by Roy and Sherrington in 1890 (13), based on the observation that brain volume increases following sensory or peripheral nerve stimulation. Since then, it has come to be accepted as a fundamental aspect of brain function. Many non-invasive brain imaging techniques used in both clinical and research settings, such as blood oxygen level dependent (BOLD) functional magnetic resonance imaging (fMRI) and positron emission tomography (PET), detect changes in blood flow as a measure of neuronal activity. Although the significance of functional hyperemia is widely accepted, the cellular mechanisms underlying this effect have not yet been well defined.

Neuronal control of blood flow. Cerebral blood vessels, both extracerebral and within the brain microcirculation, are innervated by nerve terminals (for review, see 14). The innervation of the extracerebral vasculature (for example, pial arteries), termed "extrinsic," originates from various sympathetic, parasympathetic and sensory ganglia, and can induce dilation or constriction. The sympathetic innervation is thought to be important in autoregulation of brain perfusion in the face of increased systemic blood pressure (15). No specific physiological role has yet been shown for the parasympathetic innervation, but they have been implicated in the pathology of migraine headaches (16). Sensory neurons that innervate pial vessels are activated during migraine (17), resulting in vasodilations. This is accomplished in two ways, directly by releasing calcitonin gene-related peptide (CGRP) onto the vascular muscles, but also indirectly by activating the parasympathetic system and inducing the release of

vasoactive intestinal peptide (VIP), acetylcholine (Ach) and nitric oxide (NO) from these nerve terminals (16).

The “intrinsic innervation” of blood vessels within the brain microcirculation is from neurons located in subcortical areas such as nucleus basalis (which releases Ach; 18;19), locus coeruleus (containing norepinephrine; 20) and raphe nucleus (containing serotonin; 21). Receptors for these neurotransmitters are present on the vessels, either on the smooth muscle cells themselves or on endothelial cells (14;20). ACh mediates vasodilation, while NE and serotonin mediate vasoconstriction. Although the functional effect of these subcortical innervations on the vasculature is well characterized, it is not well understood whether the effect of these substances on the vasculature is direct, or is mediated by glial cells, which also express the receptors for all three neurotransmitters involved, or a combination of the two processes. It is noteworthy that a lot of the intrinsic innervation terminates on glial endfeet, with only a small proportion terminating directly on vessels (20). Indeed a role for astrocytes was demonstrated in the NE mediated vasoconstriction recently, whereby NE stimulation induces a Ca^{2+} increase within perivascular astrocytic processes, leading to constrictions (22). While this does not preclude direct action of NE on vascular cells, it provides the first evidence that at least part of the NE induced constriction may be dependent on astrocytes. A similar role of astrocytes in mediating Ach- and serotonin-evoked vasomotion has yet to be examined.

These subcortical nuclei are known to innervate the cortical neuropil as well as microvasculature in a wide-spread manner, which implies that activation of these pathways will result in changes in blood flow over large regions of the brain. This raises the question of how local changes in blood flow are fine-tuned to match neuronal activity in that region, without influencing perfusion in other areas of the brain. Recently, a role for local interneurons in regulating cerebral blood flow has been shown (23).

Interneuron-evoked dilations appear to be mediated by VIP or NO, and constrictions appear to be mediated by somatostatin (24). As in the case of intrinsic innervations, receptors for these vasoactive molecules are present on both vascular cells as well as astrocytes (24). Whether astrocytes mediate any part of interneuron elicited vasomotor responses has yet to be investigated. Interneuron control of vasculature may be one possible mechanism for local fine-tuning of brain perfusion, as one would expect them to be activated by local neuronal activity. However, some of these interneurons are innervated by the same subcortical fibers that innervate vasculature (24), and can serve as a relay for this intrinsic innervation pathway. Thus, whether interneurons can regulate blood flow in a spatially distinct pattern to match regional neuronal activity remains an open question.

Glial cells as intermediaries between neurons and vasculature. Glial cells in the brain as well as the retina are well positioned to relay information about neuronal activity to the vascular smooth muscle cells, and their role in neurovascular coupling has been extensively investigated in the last decade. Glial cell processes contact numerous synapses from multiple neurons (25-27) and form a syncytium via gap junctions with surrounding glia. They are also capable of responding to synaptic activity, and this has been demonstrated in many regions of the brain. Electrical stimulation of the Schaffer collaterals in hippocampal slices results in a rise in intracellular calcium (Ca^{2+}) in astrocytes via activation of metabotropic glutamate receptor (mGluR) by synaptically released glutamate (28). Bergmann glial cells of the cerebellum also respond to neuronal stimulation with Ca^{2+} transients, which are induced by the activation of both glutametergic and purinergic receptors (29). Müller glial cells of the retina also exhibit Ca^{2+} transients in response to light-evoked neuronal activity, induced by activation of purinergic receptors by neuronally released ATP (30). Collectively, observations from

multiple studies throughout the central nervous system have led to the conclusion that neuronal activity can activate glial cells, which is characterized by transient intracellular Ca^{2+} increases (for review, see 31). On the other hand, glial endfeet are associated with the vasculature (32), where they ensheath blood vessels (also see Fig. 1). These morphological characteristics of glial cells, and their functional correlation with neuronal activity, make them good candidates as intermediaries between neurons and vascular cells.

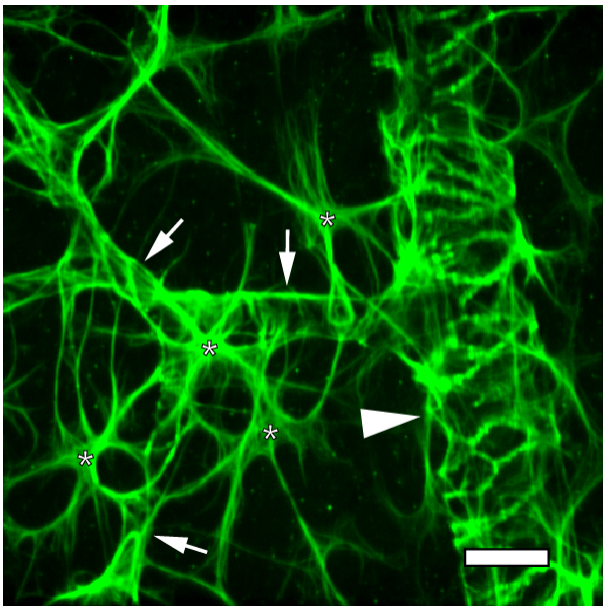

Figure 1. Whole mount retina, showing GFAP stained astrocytes (stars) with their endfeet ensheathing blood vessels. Arrowhead points to endfeet surrounding a large vessel, arrows point to endfeet surrounding capillaries. Scale bar = 10 μm.

K^+ siphoning hypothesis of neurovascular coupling. Several different mechanisms by which glial cells might regulate neurovascular coupling have been proposed. A K^+-dependent mechanism, termed "K^+ siphoning," was proposed by Paulson and Newman as far back as 1987 (33). Neuronal activity results in a rise in extracellular K^+ concentration ($[K^+]_o$) (34;35) and glial cells play a critical role in buffering this $[K^+]$ (36;37). The K^+ siphoning hypothesis states that an increase in $[K^+]_o$ (due to neuronal activity) depolarizes glial cells, which leads to K^+ efflux from glial endfeet onto blood vessels and induces vasodilation (33). This happens because small increases in $[K^+]_o$ (up to 10 mM) increases the conductance of inward rectifying K^+ channels located on vascular smooth muscle cells, effectively hyperpolarizing the smooth muscle and inhibiting the influx of Ca^{2+} through voltage-gated channels (38).

Initially, this hypothesis gained popularity and became accepted by the scientific community without any experimental evidence in support of it. It was only recently tested by directly depolarizing glial cells and monitoring vascular diameter in the *ex vivo* retina (39). Glial depolarization did not result in any changes in arteriole diameter. In addition, light stimulation of the retina in a Kir 4.1 (the channel primarily found on glial endfeet opposing vessels) knockout mouse line produced vascular responses similar to those in control animals. These findings demonstrated that the K^+ siphoning mechanism does not contribute significantly to neurovascular coupling, at least in the retina.

BK channel hypothesis of neurovascular coupling. Another K^+ based mechanism that may regulate cerebral blood flow was recently proposed by the Nelson group (40). They found that Ca^{2+} increases within glial cells evoked by neuronal activity activate large conductance Ca^{2+}-activated K^+ (BK) channels, leading to an efflux of K^+ from glial cells onto the vasculature. This rise in $[K^+]_o$ results in smooth muscle hyperpolarization, and thus dilation. This mechanism has yet to be tested in the retina and other brain regions.

The arachidonic acid metabolite hypothesis of neurovascular coupling. Ca^{2+} increase within glial cells can affect many different signaling cascades, one of them being the activation of Ca^{2+}-sensitive phospholipase A_2 (PLA_2). PLA_2 catalyzes the breakdown of membrane phospholipids into arachidonic acid (AA). Many studies have indicated that AA can be metabolized by glial cells into multiple vasoactive substances such as prostaglandins (PGs), epoxyeicosatrienoic acids (EETs) and hydroxyeicosatetraenoic acids (41;42). AA can also be released by glial cells and converted into 20- hydroxyeicosatetraenoic acids (20-HETE) in the downstream vascular smooth muscle cells (43). 20-HETE induces vasoconstriction by inhibiting Ca^{2+}-activated K^+ channels in the smooth muscle cells, resulting in depolarization and an

increase in Ca^{2+} entry via voltage gated Ca^{2+} channels (44). EETs are thought to work in the opposite manner, by enhancing K^+ conductance and thus hyperpolarizing the smooth muscle cell (44;45), although a second mechanism via inhibition of the thromboxane receptor has also been proposed (46). Prostaglandins can be either dilatory or constrictory, depending on the type of prostaglandin and the receptor it acts on. For example, PGE_2 generally induces vasodilation via the EP2 and EP4 receptors (47;48), but it can also generate vasoconstrictions via the EP1 and EP3 receptors (47;49).

The hypothesis that glial cells may regulate neurovascular coupling by releasing vasoactive AA metabolites was first proposed by Harder et al. in 1998 (50). Since then many reports have been published in support of this hypothesis. The first demonstration that EETs regulate blood flow in the brain came in 2002, when Peng et al. showed that inhibitors of epoxygenase, the synthetic enzyme for EETs, reduced functional hyperemia response to whisker stimulation *in vivo* (51). Following this, the Carmignoto (52) and Nedergaard laboratories (53) demonstrated that neuronal activity-induced vasodilations in the cortex were dependent on astrocytic Ca^{2+} increases and were inhibited by blockers of cyclooxygenase (COX), the synthetic enzyme for PGs. These studies were significant in that they demonstrated the importance of glial cells in the control of cerebrovascular tone *in vivo*.

In contrast, MacVicar's laboratory observed that raising intracellular Ca^{2+} within astrocytes-induced vasoconstrictions in hippocampal slices (22). These vasoconstrictions were induced by 20-HETE, and could be inhibited by blocking the activity of CYP4A ω-hydroxylase, the synthetic enzyme for 20-HETE. This was the first report of astrocyte induced vasoconstriction and suggested that active control of cerebral

blood flow may be a balance between dilating and constricting factors released upon stimulation.

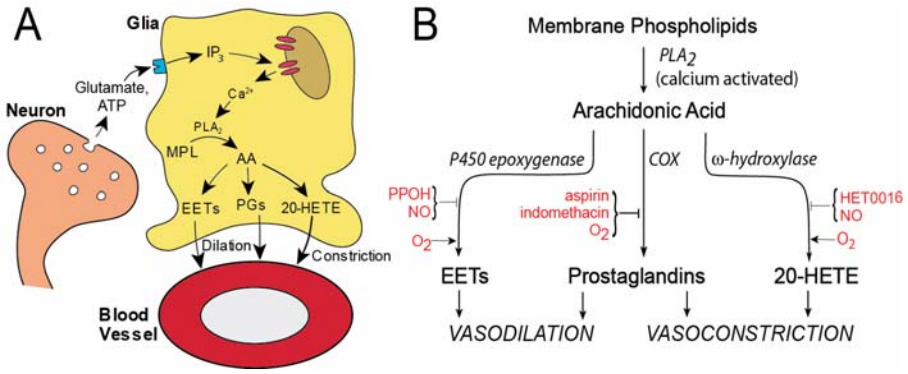

Figure 2. Arachidonic acid (AA) metabolite hypothesis of neurovascular coupling. AA is synthesized from membrane phospholipids by PLA_2 and then metabolized by downstream enzymes into multiple vasoactive compounds such as EETs, PGs and 20-HETE.

Taken together, these findings demonstrate that astrocytes do indeed, at least in part, mediate neurovascular coupling, and that this process occurs via the synthesis and release of AA metabolites, either from glial cells or downstream of them (such as in the case of 20-HETE, which is synthesized in vascular smooth muscle cells). A summary of the arachidonic acid pathways is shown in Fig. 2.

Neurovascular coupling in the retina. Neuronal activity within the retina also leads to increases in retinal blood supply, similar to those observed in the brain, and plays a prominent role in retinal function. Unlike the cerebral microcirculation, retinal vessels are devoid of autonomic innervation, precluding any regulation via these pathways (4). The retinal hemodynamic response is, instead, elicited by light-evoked activation of retinal neurocircuirty, which leads to substantial increases in retinal blood flow (3). Stimulating the retina with a flickering light (which is optimal for activating the retinal circuitry, (3)

produces large increases in retinal blood flow (~35%) with very short latencies (~1 s). Functional hyperemia in the retina is routinely monitored using multiple non-invasive techniques, such as laser Doppler flowmetry, fMRI and blue field stimulation-entoptic phenomenon observation (3). More recently, retinal vessel analysers have been used to directly measure flicker-evoked vasodilation and this method has been extensively used in the study of pathological disruption of functional hyperemia (discussed below).

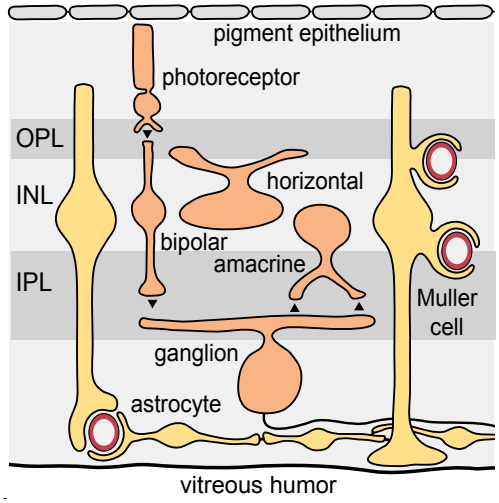

Figure 3. A schematic of the retinal circuitry. Astrocytes (on the vitreal surface) and Muller cells (spanning the width of the retina) are the two glial cells of the retina. Endfeet from these glial cells ensheath all vessels in the retina. Muller cells wrap vessels on the vitreal surface and INL, while astrocytic endfeet only ensheath the vitreal vessels.

The retina is a particularly attractive preparation in which to study the mechanisms that regulate blood flow for multiple reasons: 1) it is a projection of the central nervous system and bears similarities to cerebral microvasculature (54) and therefore many signaling mechanisms uncovered in the retina can be applied to the brain; 2) functional hyperemia is very pronounced in the retina (3); 3) the retinal surface vessels are easy to monitor both *ex vivo* and *in vivo*; 4) it can be stimulated with a physiological stimulus, light; and 5) the entire signaling network, from photoreceptors that sense light to the ganglion cells that are the output neurons of the retina, remains intact the *ex vivo* preparation and can be studied as a physiological whole (Fig. 3).

There are two types of macroglial cells in the mammalian retina: Müller cells and astrocytes (Fig. 3). Müller cells are the principle glial cells of the retina. Their somata lie in the inner nuclear layer (INL) and they extend bidirectional processes to both the photoreceptor layer and the inner surface of the retina. Astrocyte cell bodies are restricted to the vitreal surface of the retina, within the nerve fibre layer. Both Müller cells and astrocytes have endfeet processes that surround vessels. Astrocyte processes envelop the vitreal blood vessels in the inner vascular bed (Fig 1), while Müller cell processes surround blood vessels in both the inner and outer (located on either side of the inner nuclear layer) vascular beds (Fig. 3).

Previous work from the Newman laboratory showed that light-evoked neuronal activity in the *ex vivo* retina preparation induces both vasodilations and vasoconstrictions (55). Stimulation of glial cells directly, via uncaging of Ca^{2+} or IP_3, also induced similar vasomotor responses, and interfering with neuron-to-glia signaling abolished light-evoked vascular responses. In these experiments also, neurovascular coupling was found to be dependent on AA metabolites: vasoconstrictions were mediated by 20-HETE, while vasodilations were induced by the P-450 epoxygenase metabolite EET. Unlike in the brain, inhibition of COX activity did not alter neurovascular coupling in the retina in these experiments (55).

Metea and Newman also demonstrated that glial cells are necessary for neurovascular coupling in the retina. Interfering with the neuron-to-glia communication by applying blockers of purinergic receptors completely inhibited light-evoked vasomotor responses, while maintaining glial-evoked vascular responses (55).

Modulation of neurovascular coupling by NO. The finding that both dilations and constrictions can occur in the same experimental preparation in response to identical

stimuli raised the question how these responses are modulated. Metea and Newman showed that nitric oxide (NO), a known vasoactive compound, is a strong modulator of vasomotor responses in the retina (55). Light-evoked vasoconstrictions were observed when tissue concentration of NO was raised by adding NO donors to the superfusate, whereas vasodilations were observed when NO levels were decreased by adding NO synthase (NOS) inhibitors.

NO was initially discovered as an endothelium-derived relaxing factor, and is traditionally known in vascular research as a dilator (56). It accomplishes this by raising cGMP levels within vascular smooth muscle cells (57), which increase K^+ efflux, hyperpolarizing the cell and thus reducing Ca^{2+}. Metea's work demonstrated that, at least in the retina, NO can also modulate blood flow in an indirect manner (55). The exact mechanisms by which NO affects neurovascular signaling pathways are not understood yet, but it is known that NO can inhibit the both EETs and 20-HETE synthesis (44;58). The increase in light-evoked constrictions in high NO suggests that perhaps EETs synthesis in the retina is more sensitive to NO than 20-HETE synthesis, but this has yet to be proven experimentally.

Modulation of neurovascular coupling by O_2. A role for O_2 in the modulation of neurovascular coupling was also recently demonstrated in hippocampal slices (59), but another study found contradictory results *in vivo* (60), raising a controversy about whether or not O_2 modulates this response.

Because a principal role of functional hyperemia is to supply the increased demand for O_2 of active tissue, it was logical to hypothesize that O_2 may be a modulator of the signaling pathways involved in this response. The findings from MacVicar's group show that this is indeed the case in brain slices (59). They showed that glial stimulation, either

by uncaging Ca^{2+} within astrocytes or by applying mGluR agonists, results in vasoconstrictions in presence of 100% O_2, while vasodilations are generated in 20% O_2 (which results in near-physiological tissue pO_2). Lowering O_2 results in a buildup of lactate, owing to a decrease in oxidative phosphorylation and an increase in glycolysis. Lactate is then released into the extracellular space via monocarboxylate transporters (MCT). In parallel, neuronal activity results in a Ca^{2+} rise within glial cells, leading to the increased production of prostaglandin E_2 (PGE_2) which, being a phospholipid, is readily released into the extracellular space by diffusion across the lipid membrane. Extracellular concentration of PGE_2 is maintained by active uptake by the prostaglandin transporter (PGT; (61). When lactate builds up in the extracellular space, as happens in low O_2 condition, it inhibits the uptake of PGE_2 by PGT (62). This leads to PGE_2 accumulation between glial endfeet and vessels and induced vasodilation (59).

In addition, neuronal activity in low O_2 results in an increase in adenosine, which acts on vascular smooth muscle cells to inhibit constrictions. The PGE_2 pathway and the adenosine pathway interact together to increase dilations and suppress constrictions under physiological O_2 (59). In high O_2, in contrast, both lactate and adenosine levels are reduced due to increased oxidative phosphorylation, resulting in suppression of PGE_2 mediated dilations and unmasking of vasoconstrictions.

In addition to these pathways described by the MacVicar lab, O_2 can also alter neurovascular coupling by affecting the synthesis of vasoactive substances. The enzymes involved in AA metabolism are sensitive to O_2 concentration, as is NOS activity. *In vitro* experiments have shown that the K_mO_2 of nNOS is ~350 μM (approximately 266 mmHg; 63), suggesting that nNOS activity is probably low *in vivo*. Endothelial NOS activity, in contrast, is not very sensitive to O_2 (K_mO_2 of 4 μM, ~3 mmHg; 64), and would be able to contribute to vascular responses. Among the AA

metabolites, the K_mO_2 for 20-HETE production is 60-70 mmHg (65), while it is <10 mmHg for EETs production (66) and ~10 mmHg for COX activity (65). This suggests that under physiological O_2, which is ~20 mmHg in the CNS, 20-HETE synthesis would be minimal, while EETs and PG synthesis would not suffer, favoring vasodilations. In presence of high O_2, 20-HETE synthesis would increase and contribute to the vascular response, possibly inducing constrictions. Indeed, previous work from the MacVicar laboratory showed that constrictions in high O_2 were mediated by 20-HETE (22), and similar results were observed in the retina (55).

The effect of O_2 on neurovascular coupling may especially be of importance in the clinic, when patients are exposed to breathing 100% O_2. In this regard, a report from Lindauer et al. showed no effect of hyperbaric hyperoxygenation of anesthetized rats on neurovascular coupling in the cortex (60). They tested the increase in cerebral blood flow in response to electrical forepaw stimulation (a mild physiological stimuli) as well as cortical spreading depression (a strong pathological stimuli) in animals breathing normal air, 100% O_2, and 100% O_2 at 4 ATA (atmosphere absolute). No change was observed in cerebral blood flow responses in either of the high O_2 conditions, suggesting that neurovascular coupling is independent of O_2 (60).

It is important to resolve the conflicting reports of Gordon et al. (which were done *ex vivo*) and Lindauer et al. (which were done *in vivo*) on the effect of O_2 on cerebral blood flow regulation. I addressed this important issue by examining the effect of O_2 on activity-evoked vasomotor responses in the retina, both *ex vivo* and *in vivo,* and characterized the signaling pathways involved in this modulation. This series of experiments are described in detail in chapter 2.

Modulation of retinal neurovascular coupling by pathology. Disruption of functional hyperemia has been reported in multiple pathological conditions, including systemic hypertension, glaucoma, ocular hypertension and diabetic retinopathy. Flickering light-evoked arteriole dilations were reduced in hypertensive patients (67), while glaucoma patients showed a reduced response to flickering light in venules but not arterioles (68). Another study found a reduction in flicker-evoked increase in blood flow (measured by laser-Doppler flowmetry) in patients with ocular hypertension or early open angle glaucoma (69). Multiple groups have also reported a loss of flicker-evoked vasodilation, both arteriolar and venous, in diabetic patients (70-73). A reduction in functional hyperemia could deprive the active retina of oxygen and glucose, or result in an accumulation of harmful metabolites, possibly further exacerbating the pathology.

Disruption of neurovascular coupling in diabetic retinopathy. Diabetic retinopathy is a leading cause of blindness in the developed world – about 15-17% of blindness cases in Europe and the wealthier nations in the Americas are due to diabetic retinopathy (from the World Health Organization). It has traditionally been considered a disease of the retinal vasculature, characterized by capillary occlusions, microaneurysms, edema and neovascularization (reviewed in (74). Acellular capillaries and leaky vessels appear earlier in the course of disease, owing to pericyte and endothelial cell death (75).

Although the vascular pathology is pronounced in the later stages of diabetic retinopathy, it eventually leads to blindness because of neuronal damage. Recent studies conducted on animal models as well as data from post-mortem human tissue analysis have decisively demonstrated that neuronal and glial changes occur relatively early in the course of diabetic retinopathy, suggesting that non-vascular cells may also play a role in this pathology. A rise in neuronal apoptosis within the inner retina (76) and

alterations in the electroretinogram waveform can be detected soon after induction of diabetes in animal models (77). Retinal glial cells also undergo significant pathological changes (78;79). Glial reactivity, characterized by upregulation of glial fibrillary acid protein (GFAP), occurs within 3 months of diabetes (78;79). Glial cells play an important role in the regulation of extracellular glutamate by taking it up via glutamate transporters and converting it to glutamine to feed back to the neurons. This glutamate recycling is disrupted in the retinas of diabetic animals, as shown by a decrease in the conversion of glutamate to glutamine and a rise in extracellular glutamate (78).

Despite the wealth of knowledge regarding both vascular and non-vascular deficits in diabetic retinopathy, the causality between vascular pathology and neuro-glial dysfunction is still unknown (74). The findings that neuronal and glial deficits have been observed before overt vascular pathology suggest that perhaps the neuro-glial disregulation occurs first, consequently leading to the vascular changes.

Flickering light evokes a marked vasodilation in the retina and is a hallmark of retinal health. It is routinely measured non-invasively in humans (80). Interestingly, flicker-evoked vasodilation is diminished, or sometimes even abolished, in diabetic patients (70-73). This reduction in vasodilation is observed in the retinas of diabetic patients very early in the course of disease, even before any retinopathy can be detected. Such a reduction in this vascular response could starve the retina of needed oxygen and glucose, putting neurons at risk and contributing to retinal pathology. The mechanism underlying this loss of retinal functional hyperemia in diabetic patients is not understood.

Given the evidence for early glial abnormalities in diabetic retinopathy, and the role of glial cells in mediating the neurovascular coupling, a change in glia-to-vessel signaling emerges as a natural hypothesis to explain the loss of functional hyperemia in diabetes.

Moreover, inducible NOS (iNOS) expression is upregulated in diabetic retinopathy (81;82), significantly raising the NO concentration (82-84), and NO is a known modulator of neurovascular coupling in the retina (55).

I investigated functional hyperemia in retinas of diabetic animals to elucidate the signaling mechanisms by which functional hyperemia is diminished in the diabetic retina and to develop methods of reversing the loss of the vascular response. This series of experiments are described in detail in chapters 3 and 4.

Chapter 2: Oxygen modulation of neurovascular coupling in the retina

Introduction

Neuronal activity in the central nervous system (CNS) induces local increases in blood flow (5;13), a phenomenon termed functional hyperemia. Neurovascular coupling, the mechanism linking neuronal activity to changes in vascular diameter, is mediated, at least in part, by glial cells. Neuronal activity induces a rise in intracellular Ca^{2+} in glial cell endfeet surrounding vessels, which leads to the release of vasoactive arachidonic acid (AA) metabolites that induce vasomotor responses (5;22;52;53;55). Experiments in brain slices and in the *ex vivo* retina reveal that glial activation can evoke both vasodilations and vasoconstrictions. Evoked dilations are mediated by cyclooxygenase (COX) products (52;53) and epoxyeicosatrienoic acids (EETs; 51;55;85;86), while vasoconstrictions are mediated by 20-hydroxyeicosatetraenoic acid (20-HETE; 22;55).

A recent study demonstrated that neurovascular coupling is modulated by O_2 in brain slices (59). Both neuronal and glial cell stimulation elicits vasodilations in brain slices exposed to 20% O_2. In contrast, vasoconstrictions are evoked in presence of 100% O_2. However, another recent paper (60) reported the opposite effect of O_2 *in vivo*. In this study, increasing systemic O_2 by hyperbaric hyperoxygenation had no effect on cortical functional hyperemia.

The modulatory effect of O_2 on functional hyperemia is of particular interest in the clinic, where patients are often treated with 100% O_2. We now address the issue of O_2 modulation by investigating neurovascular coupling in the retina, using both *ex vivo* and *in vivo* preparations. Our results show that although O_2 profoundly modulates

neurovascular coupling in the *ex vivo* retina, there is no effect of high O_2 on neurovascular coupling *in vivo.* This discrepancy arises because the partial pressure of O_2 (pO_2) within the retina *in vivo* during hyperoxia does not rise high enough to affect neurovascular signaling pathways.

Results

We first examined the effect of O_2 on flicker-induced arteriole dilation in the *ex vivo* retina. Retinas were superfused with solutions equilibrated with either 21% or 100% O_2 and arterioles on the vitreal surface of the retina imaged with infrared differential interference contrast (IR-DIC) microscopy. In 21% O_2, light stimulation evoked vasodilation in 97.5% of vessels studied (n=40), with an average amplitude of 30.8 ± 3.7% (Fig. 1*A,C,D*). In approximately half the vessels (47.5%), the initial dilation was followed by constriction, which averaged 6.6 ± 1.4%. In 100% O_2, in contrast, only 50% of the vessels dilated in response to light stimulation (n=40; $P< 0.001$), with the average dilation reduced to 8.0 ± 2.0% ($P< 0.0001$; Fig 1B-D). The incidence of light-evoked vasoconstrictions, on the other hand, increased to 87.5% ($P< 0.001$) in high O_2 and averaged 17.3 ± 1.7% ($P< 0.005$). Oxygen did not affect the resting tone of the arterioles studied. The average resting diameter was 21.5 ± 1.5 μm in low O_2 and 22.5 ± 1.5 μm in high O_2 ($P> 0.6$). These results demonstrate that O_2 modulates neurovascular coupling in the *ex vivo* retina, in agreement with previous findings in brain slices (59).

We measured tissue O_2 tension in the *ex vivo* retina with O_2-sensitive microelectrodes to determine retinal partial pressure of O_2 (pO_2) in low and high O_2 conditions. pO_2 in retinas exposed to 21% O_2 equaled 33.6 ± 9.5 mmHg in the ganglion cell layer (Fig. 2; n=5), somewhat higher than the physiological range of 16-24 mmHg measured *in vivo* (87). When retinas were exposed to 100% O_2, pO_2 in the ganglion cell layer increased by over 16-fold to 547.7 ± 30.3 mmHg (n=7; $P< 0.0001$).

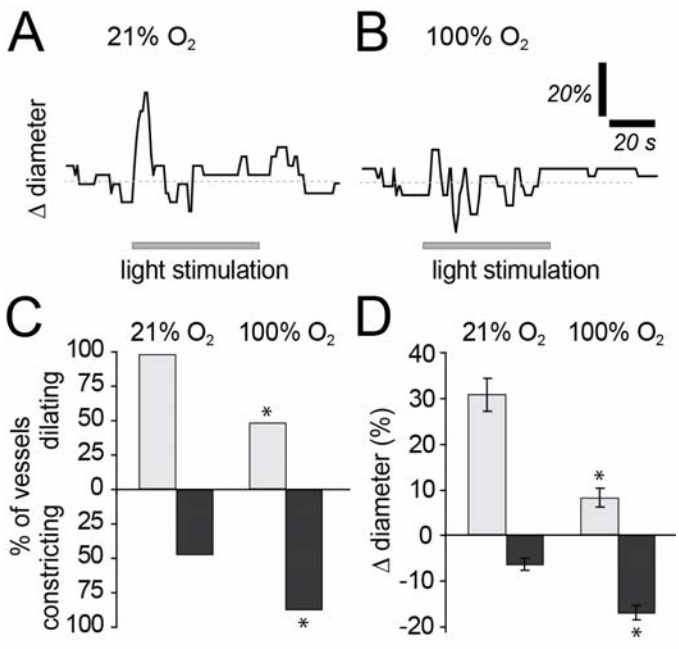

Figure 1. Light-evoked vasodilation is reduced and vasoconstriction is increased by 100% O_2 in the *ex vivo* retina. (*A*) Time course of a light-evoked arteriole response in a retina exposed to 21% O_2. (*B*) Time course of a light-evoked arteriole response in a retina exposed to 100% O_2. (*C*) The incidence of light-evoked arteriole dilations and constrictions in 21% and 100% O_2. Fewer vessels dilate and more constrict in high O_2. (*D*) The amplitude of light-evoked arteriole dilations and constrictions in 21% and 100% O_2. The amplitude of vasodilations is reduced while that of vasoconstrictions is increased in high O_2. * indicates $P< 0.005$.

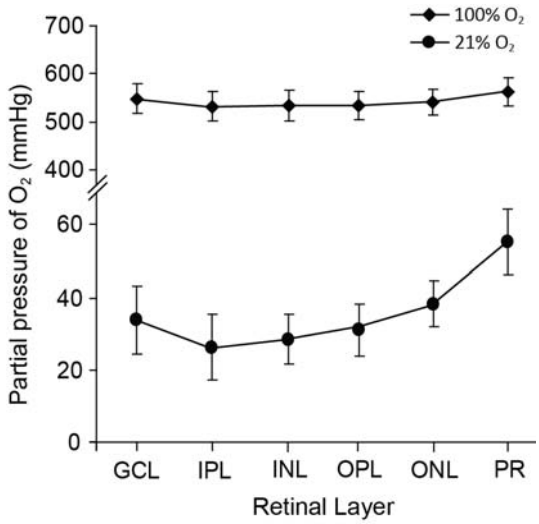

Figure 2. Partial pressure of O_2 within the *ex vivo* retina exposed to 21% and 100% O_2. Retinas perfused with 100% O_2-bubbled saline had a much higher pO_2 in all retinal layers. GCL, ganglion cell layer; IPL, inner plexiform layer; INL, inner nuclear layer; OPL, outer plexiform layer; ONL, outer nuclear layer; PR, photoreceptors.

Both prostaglandin E_2 and EETs have been implicated in mediating vasodilation in the CNS (51-53;55) and findings in brain slices indicate that the prostaglandin (PG) component is suppressed by high O_2 (59). We therefore investigated the pathways

responsible for the O_2 modulation of light-evoked vasomotor responses in the retina. We first identified vessels that dilated robustly to light stimulation, and then examined the responses of these vessels after application of inhibitors of AA metabolism. The PG pathway was tested by applying the COX inhibitors aspirin (50 μM) and indomethacin (5 μM), and the EETs pathway by inhibiting its synthetic enzyme, epoxygenase, with PPOH (20 μM). In low O_2, COX inhibition reduced light-evoked vasodilations by 81.9% (n=8; $P<$ 0.01), while in high O_2, COX inhibition had no effect (n=13; $P=$ 0.8; Fig. 3*A*). The absence of a COX-dependent vasodilating component in high O_2 arises, most likely, because the PG pathway is already suppressed by O_2. In contrast, inhibiting epoxygenase reduced the amplitude of light-evoked vasodilations in both low and high O_2. Dilations were reduced by 83.4% in high O_2 (n=7) and by 81.5% in low O_2 (n=5; $P<$ 0.05 for both; Fig. 3*A*). Inhibiting both COX and epoxygenase together also inhibited light-evoked vasodilation in both conditions, but to no greater extent than when either pathway was inhibited separately. Dilations were reduced by 77.7% in high O_2 (n=6; $P<$ 0.01) and by 87.7% in low O_2 (n=11; $P<$ 0.001; Fig. 3*A*).

These results support the view that high O_2 suppresses the PG component, but not the EETs component, of neurovascular coupling. However, they do not account for the increase in vasoconstriction observed in high O_2. The AA metabolite 20-HETE has previously been shown to mediate vasoconstrictions in both the brain and the retina (22;55) and its synthetic enzyme, ω-hydroxylase, has been proposed to be a microvascular O_2 sensor (65). We investigated the contribution of 20-HETE to vasomotor responses in the two O_2 conditions. We first identified vessels that displayed light-evoked constrictions in high O_2, and then tested their response after treatment with HET0016 (100 nM), an ω-hydroxylase inhibitor. HET0016 reduced light-evoked vasoconstrictions in high O_2 by 40.4% (n=10; $P<$ 0.05; Fig. 3*C*). In low O_2, it was not

feasible to assess the effect of HET0016 on constrictions because such responses occurred infrequently. Nevertheless, if 20-HETE is being produced and released in response to light-evoked neuronal activity, inhibiting this vasoconstrictor should result in larger dilations. However, in 21% O_2, HET0016 had no effect on the amplitude of vasodilation (n=9; *P*= 0.3; Fig. 3*B*). These results indicate that 20-HETE does not contribute to neurovascular coupling in low O_2, but mediates vasoconstrictions in high O_2.

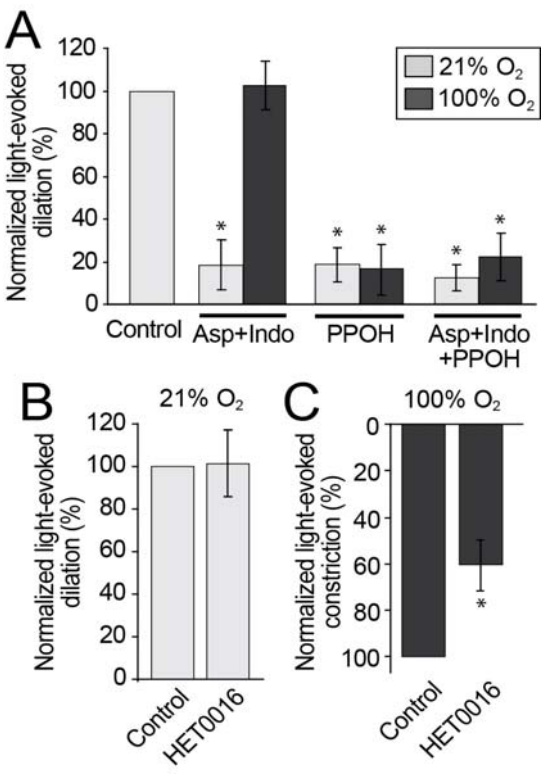

Figure 3. COX-mediated vasodilation is suppressed and 20-HETE-mediated constriction is enhanced by 100% O_2 in the *ex vivo* retina. (*A*) The COX inhibitors aspirin (50 μM) and indomethacin (5 μM) together reduced light-evoked vasodilation in retinas exposed to 21% O_2, but not to 100% O_2. The epoxygenase inhibitor PPOH (20 μM) reduced vasodilation in both low and high O_2 conditions. Aspirin, indomethacin and PPOH, applied together to block both COX and epoxygenase, inhibited vasodilation in both 21% and 100% O_2. (*B-C*) The ω-hydroxylase inhibitor HET0016 had no effect on the vascular responses observed in 21% O_2 (*B*), but reduced the amplitude of vasoconstrictions in 100% O_2 (*C*). Control and drug treatment data were collected from the same set of vessels for each inhibitor. * indicates *P*< 0.05, paired t-test.

There is accumulating evidence that neurovascular coupling is mediated, at least in part, by glia-to-vessel signaling (5). We tested whether O_2 control of neurovascular coupling occurs via modulation of glia-to-vessel signaling by observing glial-evoked vasomotor

responses in the two O_2 conditions. Glial cells were stimulated by focal ejection of ATP, which evoked Ca^{2+} waves that propagated through astrocytes and Müller cells, the macroglial cells of the retina. In low O_2, glial stimulation evoked dilations in 92.3% of the vessels, with an amplitude of 23.5 ± 4.1% (n=13; Fig. 4*A,C,D*). In high O_2, only 35.7% (*P*< 0.01) of the vessels dilated to glial stimulation, with an amplitude of 4.3 ± 1.8% (n=14; *P*< 0.001; Fig. 4*C,D*). The proportion of vessels that constricted to glial stimulation also increased from 15.4% in low O_2 to 85.7% in high O_2 (*P*< 0.01), and the amplitude of these constrictions increased from 1.5 ± 1.2% to 18.1 ± 3.1% (*P*< 0.001; Fig 4*B-D*). These data suggest that O_2 modulation of neurovascular coupling occurs by regulating glial cell-to-vessel signaling.

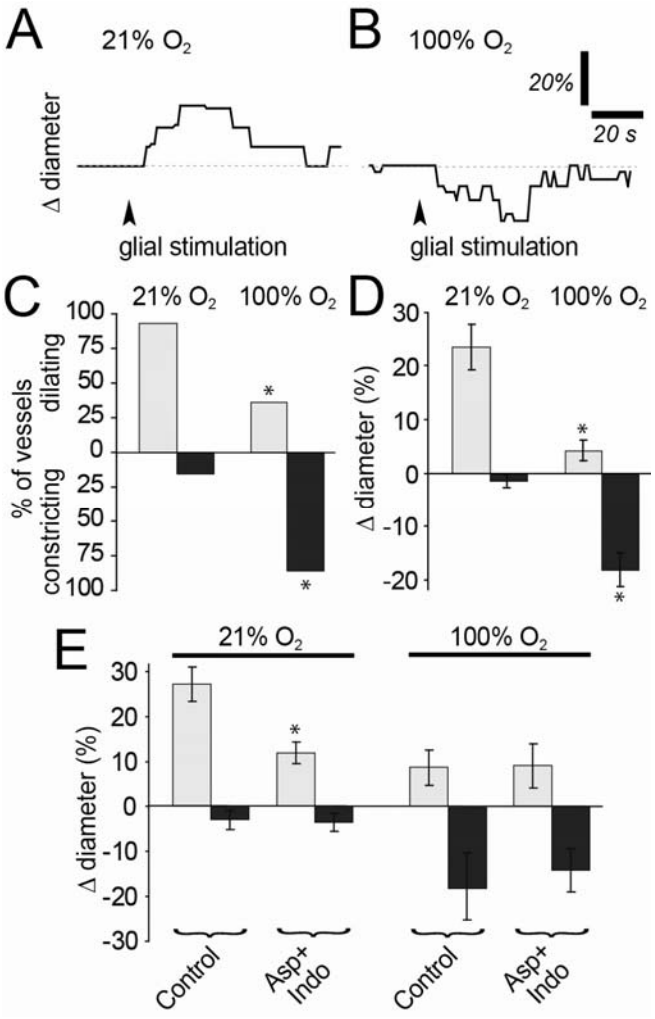

Figure 4. Glial-evoked vasodilation is reduced and vasoconstriction is increased in 100% O_2 in the *ex vivo* retina. (*A*) Time course of arteriole dilation evoked by an ATP-induced glial Ca^{2+} wave in 21% O_2. (*B*) Time course of a similarly evoked arteriole response in 100% O_2. The arteriole constricted in response to glial stimulation. (*C*) The incidence of glial-evoked vascular responses in 21% and 100% O_2. Fewer dilations and more constrictions occurred in high O_2. (*D*) The amplitude of glial-evoked arteriole dilations and constrictions in 21% and 100% O_2. Vasodilations were smaller and vasoconstrictions were larger in high O_2. (E) The COX inhibitors aspirin (50 μM) and indomethacin (5 μM) together reduced glial-evoked vasodilation in 21% O_2, but in 100% O_2. * indicates *P*< 0.01.

We tested whether the reduction in glial-evoked vasodilation we observed in high O_2 was due to a reduction of PG signaling, as was the case for light-evoked dilations. In low O_2, glial-evoked dilations averaged 27.2 ± 3.8% (n=11) in control solution, but were significantly reduced to 12.0 ± 2.4% after COX inhibition (n=11; *P*< 0.005; Fig. 4*E*).

In high O_2, in contrast, COX inhibitors had no effect. Glial-evoked dilations averaged 8.7 ± 3.9% in control solution and 9.0 ± 4.8% after drug treatment (n=6; *P* = 0.4; Fig. 4*E*). The results demonstrate that suppression of glial-evoked vasodilation in high O_2 is via the PG signaling pathway, as it is for light-evoked vasodilation.

These findings illustrate that O_2 has a substantial effect on neurovascular coupling in the *ex vivo* retina. However, it remains controversial whether O_2 has a similar modulatory effect *in vivo*. We tested this by monitoring vascular diameter and blood velocity in the retinas of anesthetized rats. When animals were switched from normoxic conditions

Table 1. Summary of physiological parameters under normoxia and hyperoxia. sO_2, arterial O_2 saturation level; pO_2, arterial partial pressure of O_2; BP, mean arterial blood pressure. * indicates *P* < 0.001.

	Normoxia	Hyperoxia
sO2	95.7± 0.5	* 98.5 ± 0.1
pO2	117± 7	* 512 ± 26
BP	118± 3	122 ± 4
pH	7.41± 0.01	7.40 ± 0.01

(arterial pO_2 = 117 ± 7 mmHg; Table 1) to hyperoxic conditions (arterial pO_2= 512 ± 26 mmHg) by artificially ventilating them with 100% O_2, there was no change in the evoked vasomotor responses. Under normoxia, diffuse flickering light stimulation evoked arteriolar dilations averaging 9.02 ± 0.9% (Fig. 5*A*) and blood velocity increases of 6.5 ± 1.6% (Fig. 5*B*). Under hyperoxia, light stimulation evoked vessel dilations of 8.84

± 1.4% (*P*> 0.8) and blood velocity increases of 7.6 ± 2.2% (*P*> 0.1), not significantly different from the normoxic responses.

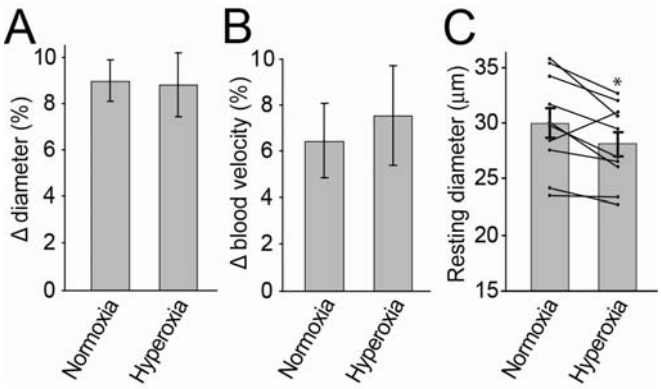

Figure 5. Effect of O_2 on light-evoked vascular responses and tone *in vivo*. (*A*) Flickering light evoked dilation of retinal arterioles in both normoxia and hyperoxia. (*B*) Flickering light evoked an increase in arterial blood velocity in both normoxia and hyperoxia. Neither the amplitude of the dilation nor the increase in blood velocity was significantly different between normoxic and hyperoxic conditions. (*C*) Resting arteriole diameter decreased after hyperoxia treatment. Bars depict average diameter of arterioles during normoxia and hyperoxia. Diameter change for individual arterioles is shown by black lines. Eight out of 10 vessels constricted during hyperoxia. * indicates *P* < 0.001 (paired t-test).

The resting tone of the arterioles, however, was significantly altered by hyperoxia. Following the switch to 100% O_2, arterioles displayed a large transient constriction followed by a partial recovery. After stabilization under hyperoxia, arteriolar diameter averaged 27.6 ± 1.1 μm, compared to the average diameter of 29.4 ± 1.4 μm in the same vessels during normoxia (*P*< 0.05; paired t-test; Fig. 5*C*). There was no change in mean arterial blood pressure between normoxic and hyperoxic conditions (Table 1).

Our results appear contradictory; high O_2 reduces neurovascular coupling substantially in the *ex vivo* retina but not *in vivo*. Resolution of this conflict may lie in differences in pO_2 within the retina in the two preparations. Our O_2 electrode measurements (Fig. 2) show that pO_2 in the ganglion cell layer of the *ex vivo* retina increases dramatically from 34 to 548 mmHg when switching from 21% to 100% O_2. In contrast, pO_2 in the ganglion cell layer *in vivo* increases only modestly from ~21 to ~53 mmHg when switching from

normoxic to hyperoxic conditions (88). This small increase in O_2 tension within the retina *in vivo* may not be sufficient to induce the modulatory changes in neurovascular coupling observed in the *ex vivo* retina.

We tested whether raising retinal pO_2 to 53 mmHg in the *ex vivo* preparation results in a modulation of neurovascular coupling. Based on our *ex vivo* pO_2 measurements (Fig. 2), we calculated that bubbling the *ex vivo* superfusate with 28% O_2 should produce a retinal pO_2 of 53 mmHg, reproducing the pO_2 level *in vivo* during hyperoxia (Fig. 6*A*). We found that the incidence and amplitude of light-evoked arteriole responses in 28% O_2 were the same as those observed in the same vessels in 21% O_2 (Figs. 6B,C). Vasodilations in 28% O_2 averaged 20.8 ± 5.4% and vasoconstrictions 10.3 ± 3.3%, compared to 21.4 ± 3.8% (P= 0.3) and 9.9 ± 2.9%(P> 0.9), respectively, in 21% O_2 (n=13). These results support the concept that O_2 modulation is absent *in vivo* because the small rise in tissue pO_2 that occurs during hyperoxia is not large enough to affect neurovascular coupling.

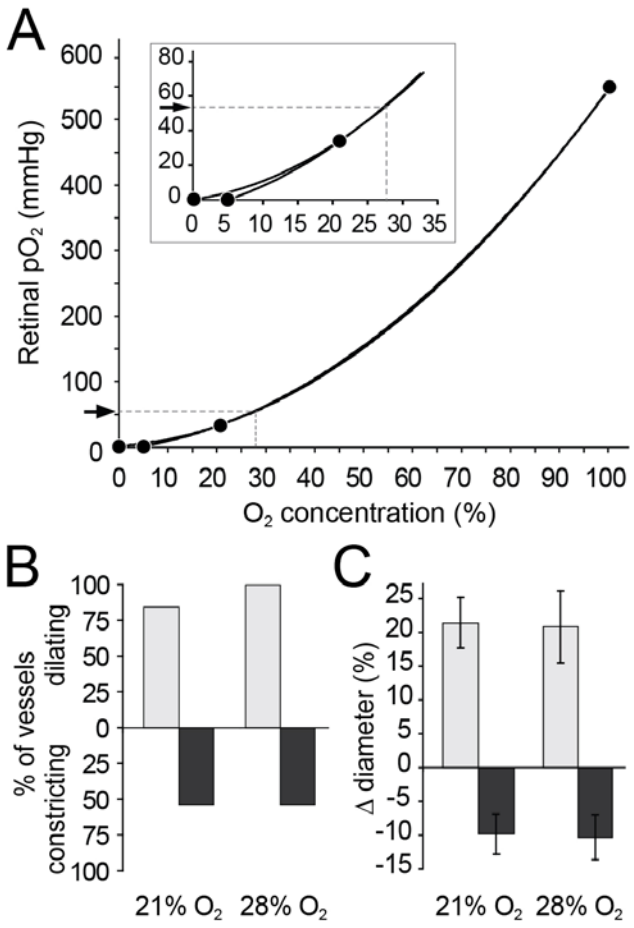

Figure 6. Raising O_2 in the *ex vivo* retina to match pO_2 in the hyperoxic *in vivo* retina has no effect on light-evoked vascular responses. (*A*) pO_2 measured in the ganglion cell layer of the *ex vivo* retina is plotted against the bubbling O_2 concentration (data from Fig. 2). The percent O_2 that yields a pO_2 of 53 mmHg (pO_2 in the hyperoxic retina *in vivo*; ref (87) in the *ex vivo* retina is estimated by interpolation (shown by dashed lines in the figure and inset). Bubbling saline with 28% O_2 results in a retinal pO_2 of 53 mmHg in the *ex vivo* preparation. The 2nd order polynomial fit is similar whether pO_2 is assumed to be zero when bubbling O_2 is 0 or 5%. (*B,C*) Neither the incidence (*B*) nor the amplitude(*C*) of light-evoked vasodilations and vasoconstrictions in the *ex vivo* retina changed when O_2 was raised from 21% to 28%. Experiments shown in B and C are from the same set of vessels.

Discussion

We have shown that in the *ex vivo* rat retina, both light- and glial-evoked vascular responses are modulated by O_2, and that this modulation is due to altered AA signaling. Both PGs and EETs mediate vasodilation under low O_2 conditions, but the contribution of PGs is absent under high O_2, causing a substantial decrease in the incidence and amplitude of light- and glial-evoked vasodilations. These results confirm the findings of the MacVicar group that, in brain slices, PG-mediated vasodilation is reduced by high O_2 (59). Their work demonstrated that high O_2 exerts its modulatory effect, in part, by altering PGE_2 transport into cells, leading to reduced extracellular PG levels under high O_2 conditions.

Oxygen also modulates 20-HETE signaling in the *ex vivo* retina. In low O_2, there is little contribution of 20-HETE to light-evoked vascular responses, but in high O_2, a substantial component of light-evoked vasoconstriction is mediated by the 20-HETE pathway. A similar 20-HETE-dependent vasoconstriction was observed previously in the *ex vivo* retina and in brain slices (22;55). Oxygen modulation of the 20-HETE pathway may be due to the O_2-dependence of 20-HETE synthesis, which has a K_mO_2 of 60-70 mmHg (65). In contrast, the K_mO_2 of COX is 10 μM (equivalent to 8 mmHg; 66) and that of EETs production <10 mmHg (65). Thus, the synthesis of PG and EETs would not be slowed nearly as much as 20-HETE at low pO_2 levels.

Oxygen modulates vasomotor responses in the *ex vivo* retina in a similar manner for both light- and glial-evoked responses, suggesting that the modulatory effect of O_2 occurs in glial cells or in downstream pathways. This is consistent with previous work demonstrating that PG is released from glial cells (41;89) and that 20-HETE synthesis occurs in downstream vascular smooth muscle cells (43).

In contrast to our *ex vivo* results, flicker-evoked vascular responses *in vivo* were not modulated by O_2. Neither arteriole vasodilation nor the increase in blood velocity changed in hyperoxia, demonstrating that blood flux did not change. Our results resolve the contradictory findings of Gordon et al. (59), who found a substantial O_2 modulation of neurovascular coupling in brain slices and Lindauer et al. (60), who found no O_2 modulation in the cortex *in vivo*. Oxygen modulates neurovascular coupling in *ex vivo* preparations because pO_2 rises dramatically (from 34 to 548 mmHg in the retina) when switching from 21% to 100% O_2. In contrast, pO_2 rises only modestly, from ~21 to ~53 mmHg, when switching from normoxic to hyperoxic conditions *in vivo* (88). Our results (Fig. 6) demonstrate that reproducing this modest rise in pO_2 in the *ex vivo* retina does not result in a change in light-evoked vascular responses. Similar small increases in pO_2 have been measured in the brain *in vivo* during hyperoxia, where pO_2 rises only to 55 - 80 mmHg (90-92). This modest increase in pO_2 likely accounts for why O_2 does not alter neurovascular coupling in the brain during hyperoxia *in vivo*.

Our results also clarify why we previously did not observe a PG component of neurovascular coupling in the *ex vivo* retina (55), although it had been reported in the brain (52;53). The earlier *ex vivo* study was conducted entirely in 95% O_2, effectively suppressing the PG component of the response.

Although hyperoxia *in vivo* did not affect functional hyperemia, it did induce a tonic vasoconstriction of retinal arterioles, confirming similar findings previously reported in both humans and animal models (93;94). This vasoconstriction could be a homeostatic response that functions to maintain a constant tissue pO_2 in the retina. An increase in vascular tone would decrease the amount of blood flowing through the tissue, and thus the amount of O_2 that is released within the retina. This vascular response may be one

reason why retinal pO_2 changes so little, despite the ~4-fold increase in arterial pO_2 observed during hyperoxia.

Oxygen, and reactive oxygen species generated in high O_2, can modulate many signaling pathways and may result in tissue damage (95). This is especially true for pathways involving heme proteins (96). The modulatory affects of O_2 should be considered when designing *ex vivo* experiments and results should be interpreted with caution, especially when tissues are exposed to high O_2. This is true not only for neurovascular studies but, more broadly, for studies involving signaling pathways in which O_2-sensitive enzymes or pathways susceptible to reactive oxygen species may play a role. For example, neuronal nitric oxide synthase is sensitive to O_2 concentration (K_mO_2 of 350 μM, equivalent to ~266 mmHg; 63), and high O_2 may alter NO-mediated synaptic regulation (64;97).

In summary, we have demonstrated that O_2 can modulate neurovascular coupling by altering AA signaling pathways. This effect is robust in the *ex vivo* retina, where tissue pO_2 rises dramatically under high O_2 conditions. The effect is not apparent *in vivo,* however, as tissue pO_2 rises only modestly, even when animals breathe 100% O_2.

Acknowledgements. We thank Serge Charpak and and Jérôme Lecoq for help with the O_2 recordings, David Attwell, Clare Howarth and Steve Sullivan for comments on the manuscript and Michael Burian for expert technical assistance. Supported by NIH EY004077, Fondation Leducq and NIH Vision Training Grant.

Materials and Methods

The *ex vivo* retina and *in vivo* rat preparations have previously been described in detail (55;98). All methods were approved by the Institutional Animal Care and Use Committee of the University of Minnesota.

Ex vivo retina experiments

Preparation. Retinas were removed from enucleated eyes of male Long-Evans rats (Harlan, Indianapolis, IN) and superfused at 2-3 ml/min with HEPES-buffered saline (in mM:128 NaCl, 3.0 KCl, 2.0 $CaCl_2$, 1.0 $MgSO_4$, 0.5 NaH_2PO_4, 15.0 D-glucose, and 20 HEPES, pH 7.4) bubbled with either air (21% O_2), 28% O_2 (balance N_2) or 100% O_2. Arterioles were pre-constricted with the thromboxane analog U-46619 (100 nM) for 10 minutes or until stable (99). Retinas were imaged with a cooled CCD camera (CoolSnap ES; Roper Scientific, Duluth, GA) and IR-DIC optics and data analyzed with MetaMorph software (Molecular Devices, Downingtown, PA). Arteriole responses were quantified as the percent change between the largest or smallest vessel diameter measured during stimulation and the average pre-stimulus resting diameter.

Retinal stimulation. For photic stimulation, diffuse flickering white light (250 ms flashes repeated twice a second for 60 s) was used. For glial stimulation, retinas were incubated in the Ca^{2+}-indicator dye fluo-4 AM (37.5 μg/ml) and pluronic F-127 (2.6 mg/ml) for 30 minutes at RT. Glial Ca^{2+} waves were evoked by focal ejection of ATP (200 μM at 10 psi for 200 ms). The ejection site was 100-150 μm in a downstream (superfusion flow) direction from a vessel to avoid any direct effects of ATP on the vessel. The ejection site location was chosen to achieve Ca^{2+} waves that propagated close to, but did not reach the vessel of interest. In low O_2, this stimulation paradigm resulted in vasomotor

responses similar to those produced by light. Glial-evoked vascular responses were obtained from a different vessel for each trial because glial cells are refractory for Ca^{2+} signaling. Glial Ca^{2+} and vessel diameter were imaged concurrently by alternate epifluorescence and IR-DIC imaging.

O_2 measurement. O_2-sensitive microelectrodes (10 μm tip diameter, Unisense, Denmark) were calibrated prior to each experiment in 0% and 21% O_2-equilibrated saline. Electrodes were advanced into the *ex vivo* retina at a 45 º angle. Retinal layers were identified by concurrent IR-DIC imaging and measurements were made when the electrode tip was centered in each layer. Recordings made while inserting the electrode closely matched those while retracting it, although only the latter were analyzed.

In vivo experiments

***Preparation*.** Surgery was performed under 2% isoflurane anesthesia. The left femoral vein and artery were cannulated for drug administration and monitoring of blood pressure, respectively, and a tracheotomy performed for artificial ventilation. During an experiment, anesthesia was maintained by infusing α-chloralose-HBC-complex (800 mg/kg bolus; 550 mg/kg/h). Animals were artificially ventilated (30–50 breaths/min) and paralyzed with gallamine triethiodide (20 mg/kg bolus; 20 mg/kg/h) to prevent eye movements. Arterial blood pressure, end-tidal CO_2, heart rate and blood O_2 saturation level (pulse oximetry) were monitored continuously. Blood gases and pH were sampled periodically. pH and mean arterial pressure were maintained within physiological limits (7.35-7.45, and 100–125 mm Hg, respectively) by adjusting the ventilation pressure and breath rate. During normoxia, inspired O_2 concentration was adjusted to maintain arterial pO_2 between 110 and 120 mmHg. Hyperoxia was induced by increasing inspired O_2 to 100%.

***Light stimulation*.** The retina was stimulated with a 12 Hz flickering diffuse white light with an illuminance of 12 klux at the surface of the globe (focused via a fiber bundle at a 45º angle).

Vascular response measurements. The retina was imaged with an Olympus FluoView 1000 confocal microscope. The luminal diameters of first order arterioles (labeled with IV injection of dextran–fluorescein) were measured with confocal line scans. Peak response was calculated as the mean of the three largest responses. Blood velocity was measured using laser speckle flowmetry (98). Data were analyzed with custom MatLab routines.

***Statistics*.** Vasomotor responses in the isolated retina were analyzed using a one-tailed Mann-Whitney-Wilcoxon rank sum test for non-normal distributions. Proportions test was used for binomial data (e.g. whether a dilation or constriction occurred: Fig 1,4,6). Homoscedastic two-tailed Student's t-test was used for pO_2 measurements *ex vivo* and physiological parameters *in vivo* (Fig 2 and Table 1). One-tailed paired t-test was used for paired data from the same vessels *ex vivo* (Fig 3) and two-tailed paired t-test was used for *in vivo* data (Fig 5). $\alpha = 0.05$ for all analysis.

Chapter 3: Inhibition of Inducible Nitric Oxide Synthase Reverses the Loss of Functional Hyperemia in Diabetic Retinopathy

Introduction

Diabetic retinopathy is a leading cause of blindness in the developed world. It has traditionally been considered a disease of the retinal vasculature. In its later stages, diabetic retinopathy is characterized by capillary occlusions, microaneurysms, edema and neovascularization (74), leading to the loss of vision in many patients. The contribution of non-vascular cells to the development of diabetic retinopathy has only recently been explored. In early stages of the disease, neurons within the inner retina die (76), and astrocytes and Müller cells (the two macroglial cells of the retina) undergo significant pathological changes (78;79). Increased apoptosis is also observed in pericytes and vascular endothelial cells (75). Although both vascular and non-vascular cells are affected in diabetic retinopathy, it is not clear whether the vascular pathology is a product or cause of the neuronal and glial dysfunction (74).

In the healthy retina, light-evoked neuronal activity leads to increased blood flow in retinal vessels. This response, termed functional hyperemia, fine tunes the retinal circulation, bringing needed oxygen and nutrients to active neurons (3). Recent studies demonstrate that functional hyperemia in both the retina and the brain is mediated, in large part, by glial cells (22;52;53;55). The release of transmitters from neurons stimulates Ca^{2+} increases within glial cells (28), leading to the activation of phospholipase A2 and the production of arachidonic acid (AA; (100). Arachidonic acid, in turn, is metabolized into a number of vasoactive compounds, including prostaglandin

E_2 (PGE_2) and epoxyeicosatrienoic acids (EETs), which dilate vessels, and 20-hydroxyeicosatetraenoic acid (20-HETE), which constricts vessels (101-103).

Two recent studies reported a dramatic reduction in functional hyperemia in diabetic patients (70;71). The loss of this vascular response could starve the retina of needed oxygen and glucose, putting neurons at risk and contributing to retinal pathology. The cellular and molecular mechanisms responsible for the decrease in functional hyperemia in diabetic patients are not known. It is possible that the neuronal or glial dysfunctions observed in early stages of the disease are responsible for altered neurovascular signaling, leading to the loss of functional hyperemia. In this study, we investigate the mechanisms underlying this loss in an animal model of diabetic retinopathy and test a treatment for restoring the response. We find that altered glia-to-vessel signaling is responsible for the loss of functional hyperemia in the diabetic retina and that inhibiting inducible nitric oxide synthase (iNOS) restores the response.

Materials and Methods

Animals. Male Long-Evans rats were obtained from Harlan (Indianapolis, IN) and treated in accordance with the guidelines of the Institutional Animal Care and Use Committee of the University of Minnesota.

Induction of diabetic retinopathy. The streptozotocin (STZ) model of type 1 diabetes (104;105) was used. Two month old rats were anesthetized with isoflurane and injected IP with streptozotocin (70 mg/kg; freshly prepared in citrate buffer). Blood glucose levels were measured three days later to ensure successful induction of diabetes (glucose > 250 mg/dl; OneTouch Ultra, LifeScan). Animals were given a low level of supplemental insulin (1.5 U of Lantus insulin glargine subcutaneously, thrice a week; 84) to prevent excessive weight loss and a catabolic response while maintaining high glucose levels. Body weight and blood glucose were monitored biweekly. Blood glucose averaged 484 $\pm$ 9 mg/dl during the survival period and 562 $\pm$ 17 mg/dl at the time of sacrifice. Vehicle-injected, age-matched controls had blood glucose averaging 139 $\pm$ 2 mg/dl during the survival period, and 204 $\pm$ 8 mg/dl at sacrifice.

Isolated retina preparation. The isolated retina preparation has been described previously (106). Briefly, animals were killed by an overdose of isoflurane and bilateral pneumothorax, and eyes enucleated. Following removal of the vitreous humor, pieces of retinas were placed in a chamber and superfused at 2-3 ml/min with HEPES-buffered saline equilibrated with air. Arterioles were pre-constricted with the thromboxane analog U-46619 (100 nM) for 10 minutes (99) or until stable to achieve comparable tone in all arterioles studied. At this concentration, U-46619 constricted arterioles moderately, rendering them responsive to both vasodilating and vasoconstricting signals. For iNOS

inhibition experiments, retinas were pre-incubated in iNOS blockers for a minimum of 90 minutes.

Retinal imaging. Retinas were imaged with a 40X water immersion objective, infrared differential interference contrast (IR-DIC) optics, and a cooled CCD camera (CoolSnap ES; Roper Scientific, Duluth, GA). Images were captured and analyzed using MetaMorph image processing software (Molecular Devices, Downingtown, PA). Techniques used to identify retinal arterioles have been previously described (55). Arteriole responses were quantified as the percent difference between the largest change in vessel diameter measured during stimulation and the average pre-stimulus resting diameter. Diffuse flickering white light (250 ms flashes repeated twice a second) was used to stimulate the retina.

Calcium Imaging and glial stimulation. Following removal of the vitreous humor, retinal pieces were incubated in the Ca^{2+}-indicator dye fluo-4 AM (37.5 µg/ml), the caged Ca^{2+} compound *o*-nitrophenyl EGTA AM (9.4 µg/ml) and pluronic F-127 (2.6 mg/ml) for 30 minutes at room temperature to selectively label retinal glia as described previously (106). Glial Ca^{2+} and vessel diameter were recorded concurrently by alternate epifluorescence and IR-DIC imaging. Photo-release of Ca^{2+} was achieved by focusing 4 ns, 5 µm diameter flashes of 337 nm UV light (VSL-337ND photolysis unit; Prairie Technologies, Middleton, WI) onto individual astrocytes or Müller cells. The UV light was pulsed 200 times at 330 Hz and repeated every second for 5 to 10 seconds until an intercellular Ca^{2+} wave was initiated.

Histology. Retinas were fixed in 4% paraformaldehyde in PBS for 1 hour. Fixed retinas were shock-frozen in a 50-50% mixture of OCT compound (Sakura Tissue-Tek) and Aquamount (Lerner Laboratories). 12 µm thick cryostat sections were cut and mounted

using Vectashield containing DAPI (Vector Laboratories). Sections were imaged using confocal microscopy.

Cell Death Detection. Apoptotic cells were detected by TUNEL labeling using the In Situ Cell Death Detection Kit, Fluorescein (Roche, Basel, Switzerland) according to the protocol provided by the supplier. Briefly, fixed sections were permeabilized in PBS containing Triton X-100 (Sigma) and then incubated in the reaction mixture for 60 min at 37º C. TUNEL positive cells were counted manually and analyzed as the number of positive cells per 10 µm segment of retinal section.

Immunolabeling. Retinal sections were blocked for 30 min with 10% normal goat serum (NGS), 0.5% Triton X-100, and 1% bovine serum albumin (BSA) in PBS, pH 7.0. All subsequent steps were conducted in PBS containing 1% NGS, 0.5% triton X and 1% BSA. Sections were stained with mouse anti-GFAP (1:500) for 1 hour at room temperature or with rabbit anti-iNOS (1:100), rabbit anti-eNOS (1:2000) or rabbit anti-nNOS (1:2000) overnight at 4º C. After washing, sections were incubated with the secondary for 1 hour at RT. Alexa-Fluor® 594 conjugated goat anti-mouse (1:400) was used for GFAP and Alexa Fluor® 488 conjugated goat anti-rabbit (1:1000) was used for all others.

Statistics. Statistical significance for vasomotor responses was determined by one-tailed Mann-Whitney-Wilcoxon rank sum test for non-normal distributions. Proportions test was used for binomial data (e.g. whether a dilation or constriction occurred). Homoscedastic two-tailed Student's t-test was used for all other analyses. α = 0.05 for all analyses.

Solutions and drugs. HEPES-buffered saline contained (in mM): 128 NaCl, 3.0 KCl, 2.0 $CaCl_2$, 1.0 $MgSO_4$, 0.5 NaH_2PO_4, 15.0 D-glucose, and 20 HEPES, pH 7.4, equilibrated with air. *o*-nitrophenyl EGTA AM, fluo-4 AM, and pluronic F-127 were from Invitrogen (San Diego, CA). 1400W (N-[[3-(aminomethyl)phenyl]methyl]-ethanimidamide dihydrochloride), U-46619 (9,11-dideoxy-9_,11_ methanoepoxyprosta5Z,13E-dien-1-oic acid), and PGE_2 (9-oxo-11α,15S-dihydroxy-prosta-5Z,13E-dien-1-oic acid) were from Cayman Chemicals (Ann Arbor, MI). Aminoguanidine hydrochloride and rabbit anti-eNOS were from Sigma-Aldrich (St. Louis, MO). Rabbit anti-nNOS and mouse anti-GFAP were from Millipore (Bedford, MA) and rabbit anti-iNOS from Santa Cruz Biotechnology (Santa Cruz, CA).

RESULTS

Light-evoked vasodilations are reduced in the diabetic retina

We first examined whether arteriole responses to light stimulation were altered in the streptozotocin (STZ) induced model of type 1 diabetes, which has been used extensively to study diabetic retinopathy (104;105). Isolated rat retinas were stimulated with diffuse flickering white light while monitoring the diameter of arterioles on the vitreal surface of the retina. Four months after induction of diabetes, light-evoked arteriole dilation was similar in diabetic (25.8 ± 4.7%; n=26 vessels) and control (22.5 ± 3.1%**;** n=11) groups. However, significant changes in neurovascular coupling were observed at seven months. At this time, light stimulation of normal retinas resulted in dilations averaging 30.9 ± 5.2% (Fig. 1*A,C***;** n=23) while dilations were reduced to 12.9 ± 1.9% (Fig. 1*B,D***;** n=19, $p < 0.001$) in diabetic retinas. Although light-evoked vasoconstrictions were rarely observed in normal retinas (4% of vessels), they occurred frequently in diabetic retinas (53% of vessels, $p < 0.005$; results summarized in Fig. 5*D,E*). Vasoconstrictions typically followed transient vasodilations (Fig. 1*D*). All subsequent experiments were conducted on seven-month survival animals.

Response differences between control and diabetic retinas could be due to differences in the resting diameter of the vessels (107). This was not the case, however. The mean resting diameter for all arterioles analyzed (after treatment with the thromboxane analog U-46619) was similar in control (25.3 ± 1.6 μm, n=52) and diabetic (26.7 ± 1.1 μm, n=85) retinas ($p > 0.4$).

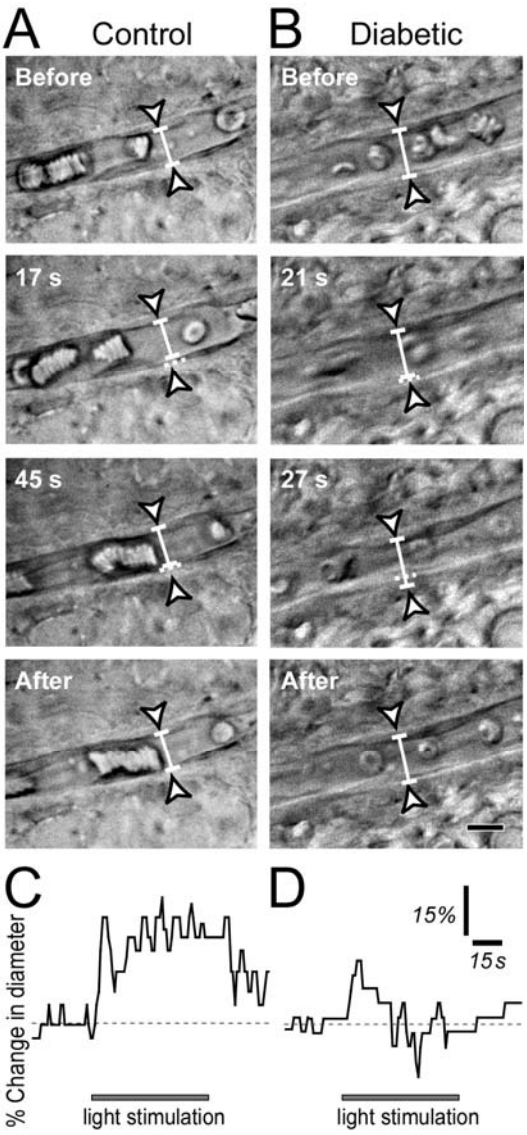

Figure 1. Light-evoked vasodilation is reduced in diabetic retinas. **A,B.** IR-DIC images of the vitreal surface of the retina, illustrating the light-evoked responses of small arterioles. In a control retina (**A**), light stimulation evokes a large vasodilation (at 17 and 45 s after onset of the light stimulus). In a diabetic retina (**B**), light evokes a smaller dilation (at 21 s), followed by a constriction (at 27 s). The diameter of both control and diabetic vessels recover to baseline after light stimulation ends. Solid white lines indicate baseline vessel diameter; dashed lines indicate changed diameter. Scale bar, 10 μm. **C,D.** Light-evoked arteriole dilation in a normal (**C**) and a diabetic (**D**) retina. Light stimulation evokes a smaller dilation, followed by a constriction, in the diabetic retina.

We questioned whether the decrease in functional hyperemia in diabetic animals was due to decreased responsiveness of retinal vessels. We tested this by directly applying the vasodilating agent PGE_2 to retinal arterioles that were responsive to light stimulation. We used a relatively high concentration of PGE_2 (200 μM) in order to evoke rapid, short latency responses. Rapid superfusion of PGE_2 produced similar dilations in control and diabetic arterioles (controls: 13 of 17 vessels dilated, 24.4 ± 19% dilation; diabetics: 10 of 11 vessels, 24.3 ± 14% dilation, $p > 0.2$; supplementary Fig. 1), irrespective of

whether they dilated or constricted to light. The results demonstrate that vascular responsiveness is not compromised in the diabetic retina.

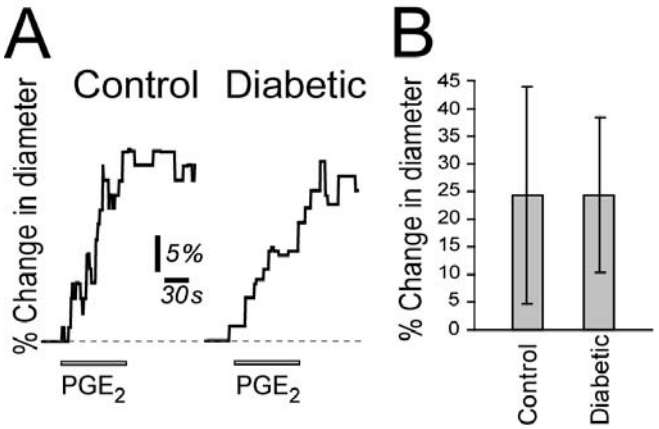

Supplementary Figure 1. Retinal arterioles in normal and diabetic retinas respond to superfusion of PGE_2 (200 μM) with similar dilations. ***A,*** PGE_2-evoked vasodilations in control and diabetic retinas. ***B,*** Summary data.

Our observation that light stimulation evokes arteriole vasodilation but rarely evokes vasoconstriction in healthy retinas differs from our previous finding (55) that stimulation typically evoked a biphasic response consisting of a transient dilation followed by a constriction. The difference in vessel behavior in the two sets of experiments is due to the oxygen levels used. Earlier experiments were performed under hyperoxic conditions (95% oxygen) while the present experiments were conducted under conditions similar to those in vivo (21% oxygen). Recent studies have demonstrated that hyperoxia blocks PGE_2-mediated vasodilation and enhances vasoconstriction mediated by 20-HETE (59;108). In the present experiments, conducted in 21% oxygen, vasodilations in healthy retinas were larger because they were mediated by both PGE_2 and EETs, while vasoconstrictions were masked.

Few overt signs of retinopathy are seen in the diabetic retina

A loss of retinal neurons, demonstrated by a decrease in the thickness of retinal layers and by increased TUNEL staining, has been reported in both diabetic patients and in

STZ-treated diabetic rats (76;109). This neuronal loss could, in theory, account for the reduction in functional hyperemia observed in our experiments. We examined whether there was a loss of neurons in our diabetic animals by measuring the thickness of retinal layers in DAPI-labeled sections (n=3 animals for controls and 4 for diabetics). There was no reduction in thickness of any of the retinal layers (Fig. 2*A*). We also examined cell death directly by TUNEL staining (Fig. 2*B,C*). There was no difference in the number of TUNEL positive cells in the control (0.17 ± 0.11 cells/mm; 2 sections each from 3 animals) and diabetic (0.13 ± 0.13 cells/mm; $p > 0.8$; 2 sections each from 4 animals) retinas. We also examined TUNEL staining 1 week after STZ injection to test whether the induction of diabetes increases apoptosis early on, as observed previously (110). We

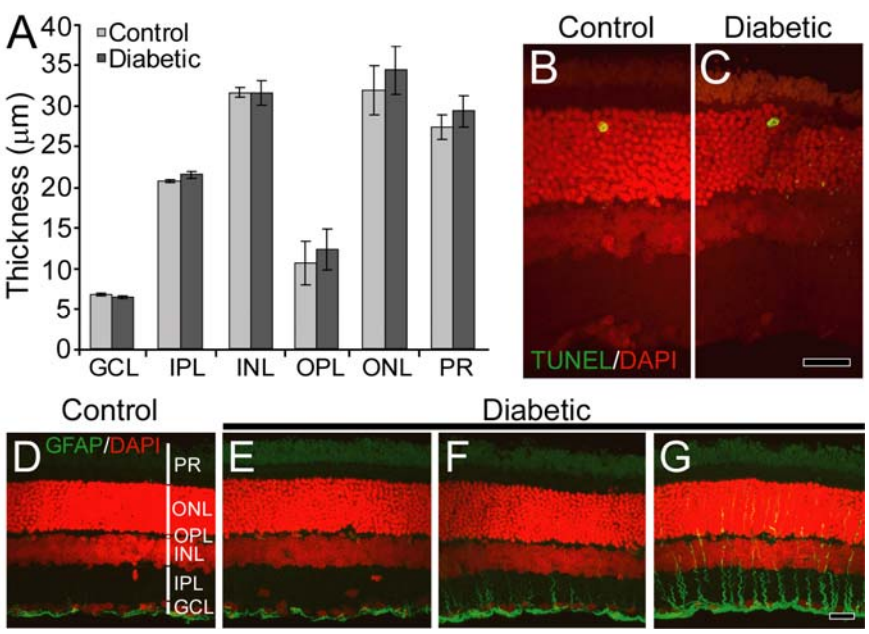

Figure 2. Few overt signs of retinopathy are seen in the diabetic retina. **A.** Mean thickness of retinal layers is not reduced in diabetic animals. GCL, ganglion cell layer; IPL, inner plexiform layer; INL, inner nuclear layer; OPL, outer plexiform layer; ONL, outer nuclear layer; PR, photoreceptors. **B,C.** Cell death was not increased in diabetic retinas. Very few TUNEL-positive cells (green/yellow profiles) were observed in both control (**B**) and diabetic (**C**) retinas. DAPI-labeled cell nuclei are shown in red. **D-G.** Immunostaining shows the expression of GFAP (green) in control (**D**) and three diabetic (**E-G**) retinas. A range of GFAP expression was observed in the vertically oriented Müller cells in diabetic retinas. Retinas from some animals were similar to controls (**E**), some showed a minor increase (**F**) while some showed substantial upregulation (**G**). GFAP-positive astrocytes, located beneath the GCL, are seen in both control and diabetic retinas. DAPI-labeled cell nuclei are shown in red. Scale bars, 20 µm.

observed no difference in TUNEL staining between controls (0.10 ± 0.05 cells/mm) and diabetics (0.07 ± 0.06 cells/mm; data not shown). These results demonstrate that there was no significant loss of neurons in our diabetic animals.

Glial-evoked vasodilations are reduced in the diabetic retina

We and others have previously shown that functional hyperemia in the retina and brain is mediated, in part, by glial cells (22;52;53;55). In this regard, it is of interest that retinal glial cells undergo pathological changes during the early stages of diabetic retinopathy. Müller cells, the principal macroglial cells of the retina, undergo an upregulation of glial fibrillary acidic protein (GFAP) and downregulation of glutamate transporters (78;79;111). We tested whether GFAP expression was upregulated in our diabetic animals. We observed an increase in GFAP expression in the Müller cells of some, but not all, diabetic animals (Fig. 2*D-G***;** n=3 controls and 4 diabetics), indicating the beginning stages of reactive gliosis.

Since the glial cells showed evidence of pathology, we reasoned that abnormal glial regulation of the vasculature could be responsible for the loss of functional hyperemia in the diabetic retina. We tested the role of glia in the loss of functional hyperemia by selectively stimulating glial cells and monitoring the resulting vasomotor responses. Glial cells (both astrocytes and Müller cells) were stimulated by raising intracellular Ca^{2+} by photolysis of *o*-nitrophenyl EGTA, a caged Ca^{2+} compound. Stimulating single glial cells evoked Ca^{2+} increases that propagated as Ca^{2+} waves into neighboring astrocytes and Müller cells (Fig. 3*A,B*). In control retinas, Ca^{2+} waves that propagated across an arteriole elicited large vasodilations averaging 36.2 ± 7% (Fig. 3*A,C***;** n=15). In diabetic retinas, these vasodilations were reduced to 15.4 ± 3% (Fig.3*B,D***;** n=13, $p < 0.02$; summarized in Fig 5*J*). In addition, glial-evoked vasoconstrictions were seen in 39% of

vessels in diabetic retinas compared to only 7% in controls, and the magnitude of constrictions was greater in diabetic animals (Fig. 5*I,J*). The decrease in glial-evoked vasodilations and increase in vasoconstrictions were not due to reduced glial cell activation. Photolysis of caged Ca^{2+} produced similar glial Ca^{2+} increases in control and diabetic retinas (controls: $\Delta F/F = 15.9 \pm 1.7\%$; diabetics: $13.3 \pm 1.9\%$, $p > 0.3$; Fig. 5*K*). These results indicate that the deficit in functional hyperemia seen in diabetic retinas is likely due to compromised glial regulation of vessel diameter.

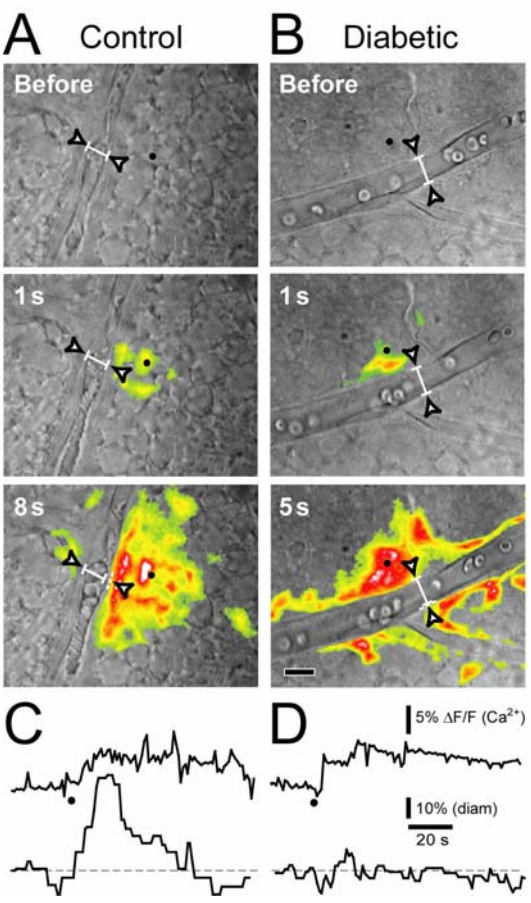

Figure 3. Glial-evoked vasodilation is reduced in diabetic retinas. **A,B.** IR-DIC images of a normal (**A**) and diabetic (**B**) retina showing small arterioles. Pseudocolor images showing glial Ca^{2+} increases are superimposed. In **A** and **B**, the top two images show time points before and 1 s after photolysis of caged Ca^{2+} in single glial cells (black dots). The last images show time points at which maximum vessel dilation was observed, with maximum $\Delta F/F$ Ca^{2+} projections overlaid. Although the glial Ca^{2+} increases are similar in control and diabetic retinas, the glial-evoked dilation is smaller in the diabetic retina. Scale bar, 10 μm. **C,D.** Ca^{2+} increases (upper traces) and arteriole diameters (lower traces) in a control (**C**) and a diabetic (**D**) retina. Photolysis of caged Ca^{2+} (black dots) produces similar glial Ca^{2+} increases in control and diabetic retinas. Yet, glial stimulation produces smaller arteriole dilations in the diabetic retina.

iNOS is upregulated in the diabetic retina

We have previously shown that nitric oxide (NO) is a modulator of functional hyperemia in the retina (55). Both light stimulation and glial cell stimulation evoke vasodilations when NO levels are low. Vasodilations are reduced and vasoconstrictions are enhanced, however, when NO levels are raised. Notably, iNOS expression is increased and tissue NO concentration is raised in the retinas of diabetic animals (84;112). We confirmed that iNOS was upregulated in our diabetic retinas by immunohistochemistry, which indicated an increase in iNOS levels in the ganglion cell, inner plexiform and outer nuclear layers (Fig. 4*A-D*; n=3 controls and 4 diabetics). iNOS was expressed in retinal glia as well as neurons. No changes in the expression of neuronal or endothelial NOS were observed (Fig. 4*E-L*).

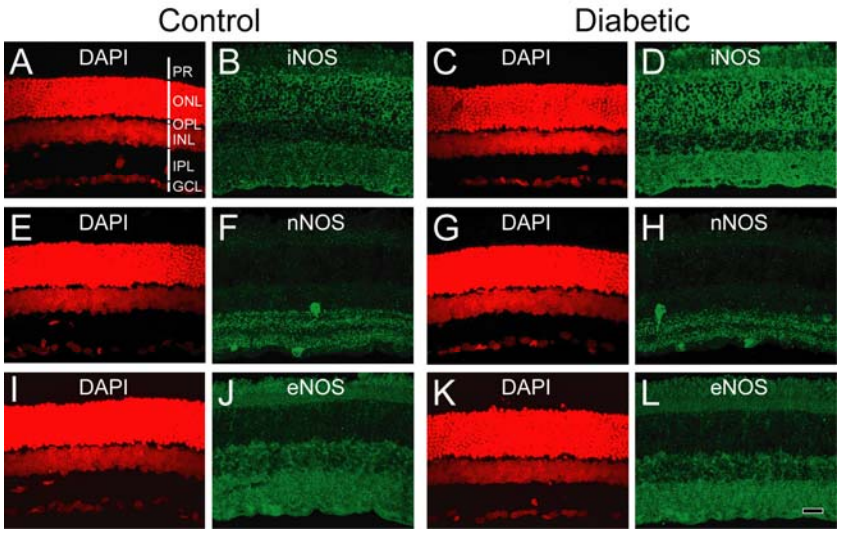

Figure 4. iNOS expression is increased in diabetic retinas. Immunostaining shows the expression of iNOS, nNOS and eNOS (green) in control (**B,F,J**) and diabetic (**D,H,L**) retinas. DAPI staining (red) shows cell nuclei in control (**A,E,I**) and diabetic (**C,G,K**) retinas. iNOS expression in the ONL, IPL and GCL of diabetic retinas (**D**) is raised compared to controls (**B**). nNOS (**F,H**) and eNOS (**J,L**) expression is unaltered in diabetic retinas. Scale bar, 20 μm.

Inhibition of iNOS restores light-evoked and glial-evoked vasodilations

We reasoned that increased NO levels in the inner retina due to the upregulation of iNOS might be responsible for reduced functional hyperemia in diabetic animals. We tested this by treating diabetic retinas with 1400W and aminoguanidine, two inhibitors of NOS that are relatively selective for iNOS at the concentrations used. In the presence of either 1 μM 1400W or 100 μM aminoguanidine, the amplitude of light-evoked vasodilations in diabetic retinas was restored to control levels (Fig. 5*A-E*; 1400W: 27.3 ± 3.5%, n=22: aminoguanidine: 28.3 ± 2.7%, n=26; neither different from controls, $p > 0.3$). The incidence and amplitude of light-evoked vasoconstrictions, which were raised in diabetic retinas, were also reduced to control levels by the iNOS inhibitors (Fig. 4*D,E*). 1400W had no effect on light-evoked vasomotor responses in control retinas (28.4 ± 5%, n=15, $p > 0.4$; supplemental Fig. 2), suggesting that NO synthesized by iNOS does not play a significant role in neurovascular coupling in healthy retinas.

If increased NO levels reduce functional hyperemia in the diabetic retina by interfering with glial control of vessel diameter (55), then inhibiting iNOS should restore glial-evoked vasodilations as well in diabetic animals. This proved to be the case. In the presence of aminoguanidine, glial-evoked vasodilations were restored to control levels in diabetic retinas (27.4 ± 9%, n=5, $p > 0.2$ compared to controls) and no glial-evoked vasoconstrictions were observed (Fig. 5*F-J*). Aminoguanidine did not alter the photolysis-evoked glial Ca^{2+} response (Fig. 5*K*).

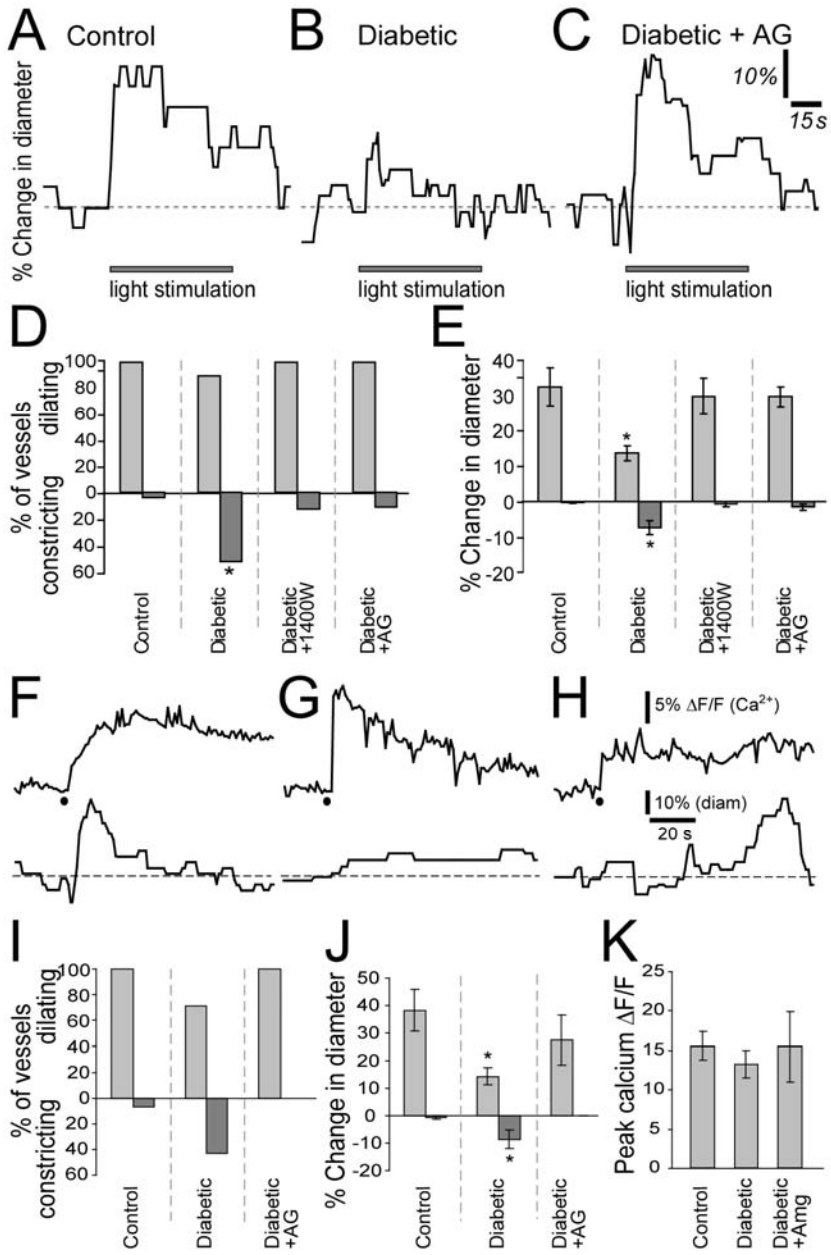

Figure 5. Inhibition of iNOS activity restores light- and glial-evoked vasodilation in diabetic retinas. **A-C.** Light-evoked vasomotor responses in a control retina (**A**), diabetic retina (**B**) and a diabetic retina treated with aminoguanidine (AG, 100 μM; **C**). **D**. The incidence of light-evoked arteriole dilations and constrictions. The incidence of vasoconstrictions is increased in diabetic retinas and is restored to control levels by 1400W (1 μM) and AG (100 μM), two inhibitors of iNOS. **E.** The magnitude of light-evoked arteriole dilations and constrictions. The magnitude of vasodilations is reduced while that of vasoconstrictions is increased in diabetic retinas. 1400W and AG restore these vasomotor responses to control levels. **F-H.** Photolysis-evoked glial Ca^{2+} increases (upper traces) and the resulting vascular responses (lower traces) in a control retina (**F**), diabetic retina (**G**) and a diabetic retina treated with AG (100 μM; **H**). Black dots indicate photolysis of caged Ca^{2+}. **I.** The incidence of glial-evoked arteriole dilations and constrictions. **J**. The magnitude of glial-evoked vasodilations and constrictions. The magnitude of vasodilations is reduced and vasoconstrictions increased in diabetic retinas. Both are restored to control levels by AG. **K.** Photolysis-evoked peak glial Ca^{2+} responses (measured in processes surrounding vessels) are not different between control, diabetic and AG-treated diabetic retinas. * $p > 0.3$.

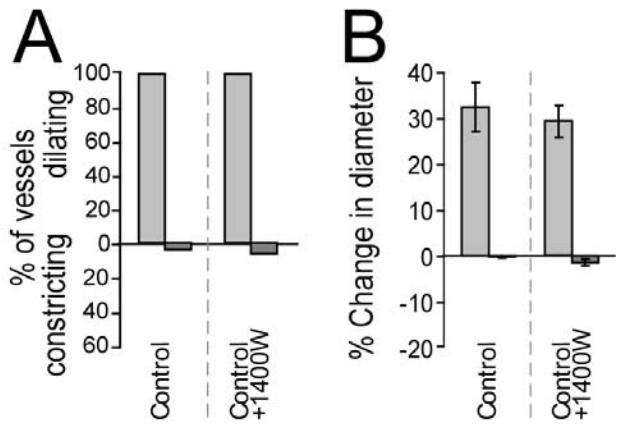

Supplementary Figure 2. iNOS inhibition by 1400W (1 μM) does not alter light-evoked vasodilation in control retinas. Neither the incidence ***(A)*** nor the magnitude ***(B)*** of light-evoked vasomotor responses was changed by 1400W.

DISCUSSION

Our results demonstrate that the STZ rat model of diabetes reproduces the deficit in functional hyperemia observed in diabetic patients. Light-evoked vasodilations in the isolated retina are significantly reduced in diabetic animals. This deficit is not due to a loss of retinal neurons or vascular responsiveness, but rather is due to aberrant glia-to-vessel signaling. Notably, the loss of functional hyperemia can be restored by aminoguanidine and 1400W, two inhibitors of iNOS.

The diabetic retinas used in our study showed few overt signs of retinopathy. Although functional hyperemia was reduced and iNOS expression increased, there was no loss of retinal neurons or any evident changes in the morphology of the vasculature. In contrast, several previous studies have reported alterations in neuronal function, changes in the expression patterns of neurons and glial cells, and neuronal and vascular cell death in early diabetic retinopathy (reviewed in 74). Most of these studies were conducted using Sprague Dawley or other albino rat strains, which are susceptible to light-induced retinal damage. Our study, in contrast, used pigmented Long-Evans rats. It is likely that albino strains show a higher level of retinopathy when made diabetic due to the added effect of light damage. Indeed, a recent study demonstrated that albino Sprague Dawley rats showed a large increase in inflammatory cytokines four months after STZ treatment while pigmented rats (Long-Evans and Brown Norway) showed only small increases in just a few of their measures (113). Moreover, in STZ-treated pigmented mice, neuronal cell death did not differ from controls for up to a year after an initial transient increase in apoptosis (110). The lack of overt retinal pathology at 7 months in our diabetic animals is, we believe, due to pigmented eyes being less vulnerable to damage.

Our observation that glial-evoked and light-evoked vasodilations were similarly reduced in diabetic retinas suggests that the loss of functional hyperemia was not due to altered neuronal responses to light stimulation. In addition, inhibition of iNOS restored both light- and glial-evoked dilations to control levels, arguing against any significant neuronal dysfunction. It is likely that changes in glial cell signaling to the vasculature underlie the deficits in functional hyperemia that we observed.

iNOS is upregulated in response to injury and pathology in many systems (114). In diabetic retinopathy, iNOS is upregulated in retinal neurons and glial cells and retinal NO levels are raised (84;112). We have confirmed that iNOS is upregulated in our model of diabetic retinopathy. Immunolabeling for iNOS, but not nNOS or eNOS, was increased in retinal glial cells and neurons. Although iNOS was upregulated in our diabetic animals, mean arteriole diameter after treatment with the thromboxane analog U-46619 was no larger in diabetic than in control retinas. This is not surprising, as NO has multiple effects on the neurovascular unit. In addition to directly dilating vessels by raising cGMP levels in vascular smooth muscle cells (57), NO can also inhibit glial production of vasodilating EETs compounds (44;58).

Our finding that iNOS inhibitors restore both light- and glial-evoked vasodilation indicates that raised NO levels are responsible for the loss of functional hyperemia, most likely by disrupting glial signaling to vessels. We have previously shown that vasodilation in the retina is mediated by glial release of EETs and PGE_2 (55;108) and that raised NO levels reduce vasodilation and enhance vasoconstriction (55). It is likely that NO reduces vasodilation by inhibiting glial production of EETs (44;58), although this has yet to be tested in the retina.

The STZ rat model of type I diabetes replicates many of the pathologies associated with human diabetic retinopathy (104). However, there are several limitations to this model that should be kept in mind. First, the timeline of disease progression is very different in the STZ rat model, which progresses over months, and type I diabetes in patients, which can take well over a decade to develop (78;115). Second, blood glucose levels are poorly controlled (intentionally) in our model, while they are well controlled in most patients diagnosed with diabetes. Additionally, the observations made in our model of type I diabetic mellitus may not be directly applicable to type II diabetes, even though retinopathy can develop in both cases, and therefore should be interpreted with care.

The loss of functional hyperemia is one of the first deficits observed in our diabetic retinas. Reduced vasodilation in response to neuronal activity will create a mismatch between energy supply and demand, depriving neurons of oxygen and nutrients (116). This disparity may be an important contributing factor in the development of diabetic retinopathy (104). Restoring functional hyperemia by inhibiting iNOS may slow progression of the pathology. Indeed, aminoguanidine (which also inhibits the formation of advanced glycation end-products; (117), has been shown to prevent transcriptional, morphological and ultrastructural changes in the retina in diabetic animals (82;118;119). Thus, the use of iNOS inhibitors such as aminoguanidine hold promise in treating diabetic retinopathy and should be explored in future studies.

Acknowledgements. We thank Alfonso Araque, Brian MacVicar and Anja Srienc for helpful discussions and comments on the manuscript, and Michael Burian for technical assistance. Supported by NIH EY004077, Fondation Leducq and NIH Vision Training Grant.

Chapter 4: Aminoguanidine Reverses the Loss of Flicker-induced Vasodilation in a Rat Model of Diabetic Retinopathy

Introduction

Diabetic retinopathy, a leading cause of blindness in the developed world, has a complex pathology that affects both neuronal and vascular elements of the retina (74-76;120). In the healthy retina, flickering light induces dilation of retinal vessels by a process termed neurovascular coupling, bringing additional oxygen and nutrients to meet the increased metabolic demands of active neurons (3;80). A reduction in this vascular response is one of the earliest retinal changes observed in diabetic patients (70-73). Although the cause, and the possible consequences, of this reduction in flicker-induced vasodilation are not known, such a reduction could deprive the active retina of oxygen and glucose, and possibly contribute to the development of diabetic retinopathy.

We previously studied neurovascular coupling in a rat model of streptozotocin-induced type 1 diabetes. Using an *ex vivo* retina preparation, we observed a reduction in flicker-induced arteriole dilation in these diabetic rats, paralleling the findings in diabetic patients (121). We found that inducible nitric oxide synthase (iNOS) was upregulated in these diabetic retinas, and inhibiting iNOS with aminoguanidine (AG; 122) or 1400W restored flicker-induced vasodilation. The results from these *ex vivo* experiments suggest that deficits in neurovascular coupling can be reversed.

AG, one of the drugs we used to inhibit iNOS, has been previously shown to slow the progression of diabetic retinopathy in humans and in animal models of diabetes (123;124). The beneficial effects of AG have largely been attributed to the inhibition of

advanced glycation end-product (AGE) formation, but our previous findings, and those from other studies, suggest that AG could also be acting by inhibiting iNOS (112;121;123), especially in early stages of the disease.

We have now examined whether AG can reverse the disruption of neurovascular coupling in the retinas of diabetic rats *in vivo*. We find that flicker-induced arteriole dilation is substantially reduced in diabetic rat retinas, as it is in patients with diabetic retinopathy. This reduction can be reversed by administering AG to diabetic rats, either acutely via IV injection or long-term in drinking water.

Materials and Methods

Induction of diabetes. Male Long-Evans rats (Harlan, Indianapolis, IN) were housed and treated in accordance with the guidelines of the ARVO Statement for the Use of Animals in Ophthalmic and Vision Research and the Institutional Animal Care and Use Committee of the University of Minnesota. Diabetes was induced as previously described by injecting two month old anesthetized rats with streptozotocin (70 mg/kg, IP; freshly prepared in citrate buffer; 121) Successful induction of diabetes, defined as blood glucose > 250 mg/dl (OneTouch Ultra, LifeScan, Milpitas, CA), was tested 3 days later. Animals were given a low maintenance dose of supplemental insulin (1.5 U Lantus insulin glargine subcutaneously, thrice a week) to prevent excessive weight loss and a catabolic response while maintaining high glucose levels (84). Body weight and blood glucose were monitored biweekly. Blood glucose during the survival period averaged 535 $\pm$ 16 mg/dl for diabetic rats and 543 $\pm$ 12 mg/dl for diabetic rats treated with AG in drinking water.

***In vivo* rat preparation.** The *in vivo* rat preparation has been described previously (98). Surgery was performed under 2% isoflurane anesthesia. Core body temperature was continuously monitored and maintained at 37 ºC (TC-1000 Temperature Controller, CWE, Ardmore, PA). The left femoral vein and artery were cannulated for drug administration and monitoring of blood pressure, respectively, and a tracheotomy performed for artificial ventilation. The animal was placed in a modified stereotaxic holder with a three-point head restraint. An IV bolus of atropine (0.1 mg/kg) was delivered prior to any eye manipulations to counter the oculocardiac reflex, which can reduce blood pressure. The right pupil was dilated with 1% atropine sulfate. Corneal refraction was neutralized by placing gonioscopic prism solution and a contact lens

(5.4 mm fundus laser lens, Ocular Instruments, Bellevue, WA) over the cornea. The stereotaxic holder containing the rat was fixed to a movable stage below an upright microscope.

Anesthesia was maintained for the duration of the experiment by continuously infusing α-chloralose-HBC-complex (55 mg/kg/h). Animals were artificially ventilated (30–50 breaths/min; CWE SAR-830-P) and paralyzed with gallamine triethiodide (20 mg/kg bolus; 20 mg/kg/h) to prevent eye movements. Arterial blood pressure (Pressure Monitor BP-1, World Precision Instruments, Sarasota, FL), end-tidal CO_2 (microCapStar, CWE), and blood oxygen saturation level and heart rate (MouseOx, Starr Life Sciences Corp, Oakmont, PA) were monitored continuously. Blood gases and pH were sampled periodically (Instrumentation Laboratory Gem Premier 3000, Radiometer, Westlake, OH). Blood oxygen saturation, pH and mean arterial pressure were maintained within physiological limits (92–97%, 7.35-7.45, and 100–125 mm Hg, respectively) by adjusting the ventilation pressure, breath rate and inspired O_2 concentration.

Light stimulation. Retinal photoreceptors were stimulated with a flickering diffuse white light at 12 Hz, a frequency that evokes a maximal vascular response (3). Light from a fiber optic illuminator was gated with an electromechanical shutter and focused onto the globe at a 45º angle through a fiber bundle. The illuminance of the light was 12 klux at the surface of the globe.

Measurement of flicker-induced dilation. The retina was imaged through the contact lens, cornea and lens of the eye with a 4X objective and an Olympus FluoView 1000 laser scanning confocal microscope (Melville, NY). Blood vessels were labeled by IV injection of dextran fluorescein isothiocyanate (2,000,000 MW, 3% solution, 1-3 ml). The luminal diameters of first order arterioles were measured with confocal line scans drawn

perpendicular to the vessel (98) and luminal diameter vs time graphs calculated with a custom MatLab routine. Flicker-induced dilations were composed of transient and sustained phases. Response amplitude was measured using the first transient peak. For each animal, the peak response was calculated as the mean of the three largest responses.

Electroretinogram (ERG) measurement. The corneal ERG electrode was attached to the center of a custom-made plastic light diffuser, which was placed over the cornea. The reference electrode was placed under the skin on the right cheek, 1 cm from the eye. The retina was dark-adapted for 15 min prior to recording ERGs. 10 ms flashes of diffuse white light were focused onto the diffuser. A series of flashes (intensities -3 to 0 log units) was employed to determine the ERG b-wave intensity-response relation. The 0 log unit stimulus had an illuminance of 120 klux at the surface of the diffuser. ERGs were averaged to improve signal-to-noise ratio. Animals displaying noisy ERGs were excluded from analysis. ERGs were filtered (1-100 Hz bandpass) and b-wave amplitude was measured from the negative a-wave trough to the positive b-wave peak.

Chemicals. Streptozotocin, aminoguanidine hydrochloride, α-chloralose-HBC-complex, gallamine triethiodide and dextran fluorescein isothiocyanate were purchased from Sigma (St Louis, MO), lantus insulin glargine from sanofi-aventis U.S. (Bridgewater, NJ), atropine for IV administration from Baxter (Deerfield, IL) and for topical application from Alcon Laboratories (Fort Worth, TX).

Statistics. Homoscedastic one-tailed Student's t-test was used for all comparisons between control and diabetic animals. Homoscedastic two-tailed Student's t-test was used for comparisons between treated and untreated control animals. Data are presented as mean ± SEM. $\alpha = 0.05$ for all analyses.

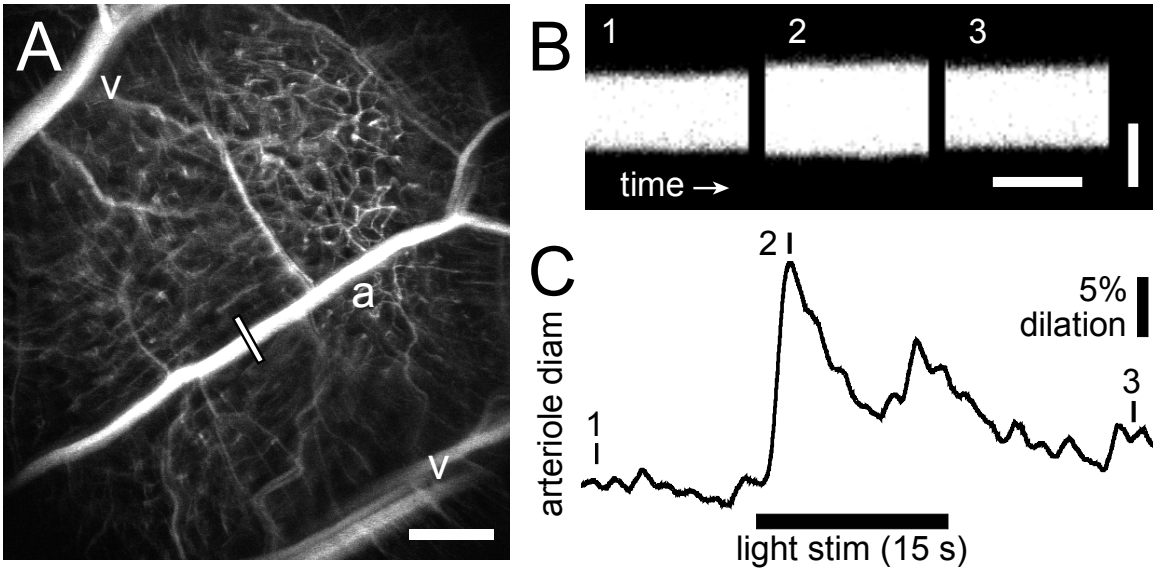

Figure 1. Measurement of flicker-induced changes in retinal arteriole diameter using confocal line scans. (A) Low power confocal image of retinal vessels. Arterioles (a) can be distinguished from venules (v) by their branching pattern and relative size. The diameter of the arteriole was measured with confocal line scans (white line). Scale bar, 250 μm. (B) Segments of a line scan image from the arteriole in A. The vertical bars in C indicate the times at which the 3 segments were taken. Distance is represented vertically (scale bar, 25 μm) and time horizontally (scale bar, 100 ms). A diffuse flickering light evoked vessel dilation, indicated by the widening of the vessel in segment 2. (C) Time course of the flicker-induced arteriole dilation. The onset of the flickering light (black bar at bottom) evoked an initial transient dilation followed by a smaller secondary dilation.

Results

We evaluated flicker-induced retinal arteriole dilation *in vivo* in diabetic and age-matched control rats. Experiments were conducted after a 7 month survival period, at which time there is a significant reduction in flicker-induced arteriole dilation in the *ex vivo* retina (121). The retina was stimulated with a diffuse 12 Hz flickering light and the luminal diameter of arterioles measured with confocal line scans (Fig. 1). In age-matched control animals, light stimulation evoked pronounced arteriole dilations composed of an initial transient dilation followed by a sustained response (Fig. 2). Flicker-evoked dilations in control retinas averaged 10.8 ± 1.1% (n = 7). The dilatory response was greatly diminished in diabetic animals (Fig. 2), where responses averaged 4.2 ± 0.3% (n = 6), only 39% of control responses ($P < 0.0001$; summarized in Fig. 3A).

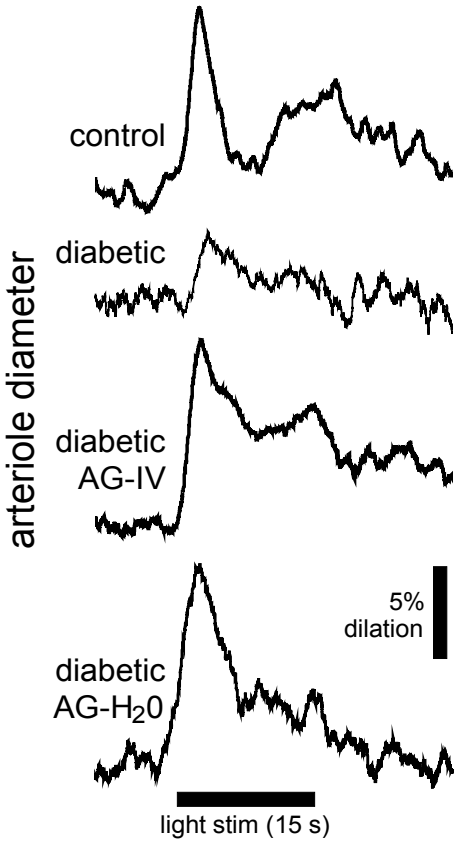

Figure 2. Flicker-induced dilation of retinal arterioles in control and diabetic animals. A diffuse flickering light (black bar at bottom) evoked a prominent arteriole dilation in a control animal, but a much smaller dilation in a diabetic animal. Treatment with the iNOS inhibitor AG restored flicker-induced arteriole dilations in diabetic animals to control levels when given intravenously (diabetic AG-IV), or in drinking water (diabetic AG-H_2O).

We showed previously in the *ex vivo* retina that increased tissue concentration of nitric oxide (NO), resulting from iNOS upregulation, was responsible for the reduction in flicker-induced dilations. We were able to reverse this loss by inhibiting iNOS (121). We have now evaluated the effect of the iNOS inhibitor AG on flicker-induced arteriole dilations *in vivo*. AG was administered in two ways. We intravenously injected AG (100 mg/kg) to test the effect of acute AG treatment. Flicker-induced changes in arteriole diameter were measured within 4 hours of AG injection. We also tested the effect of long-term AG treatment by adding AG to the drinking water of diabetic rats (500 mg/L; (118) starting 1 week after successful induction of diabetes and continuing for the duration of the survival period. Both treatment paradigms reversed the loss of flicker-induced arteriole dilation in diabetic animals (Fig. 2). Flicker-induced dilations in the AG treatment groups averaged 8.8 ± 0.9% (n = 3) for IV administration and 9.5 ± 1.3% (n = 7) for drinking water administration, both significantly larger than in untreated diabetic rats ($P < 0.002$; Fig. 3A). Neither treatment group was different from controls ($P > 0.2$).

AG treatment could affect flicker-induced dilations in controls animals, but this was not the case in our experiments. AG administration, both IV and in drinking water, had no effect on flicker-induced dilations in controls (10.0 $\pm$ 0.8%, n = 7 and 9.6 $\pm$ 0.4%, n = 6, respectively, $P > 0.3$; Fig. 3B). AG was administered in drinking water for two months prior to experiments.

The loss of neurovascular coupling observed in diabetic animals could be due to a change in the resting diameter of the arterioles. Vessels that are more dilated at rest would not be able to dilate as much in response to light. However, there was no difference in the resting arteriole diameter between groups in our study. The resting diameter of retinal arterioles was 32.7 $\pm$ 1.4 μm (n = 7) in control animals, 35.6 $\pm$ 2.0 μm

(n = 6) in diabetic animals ($P > 0.1$), and 29.3 ± 7.6 µm (n = 3; $P > 0.2$) and 34.8 ± 2.1 µm (n = 7; $P > 0.2$) in diabetic animals treated with AG IV and in drinking water, respectively (Fig. 3C). Control animals treated with AG in drinking water had a slightly larger mean resting diameter (37.9 ± 1.8 µm, n = 6; $P = 0.04$), while IV injection of AG had no effect (34.5 ± 2.1 µm, n=7; $P > 0.4$; Fig. 3D).

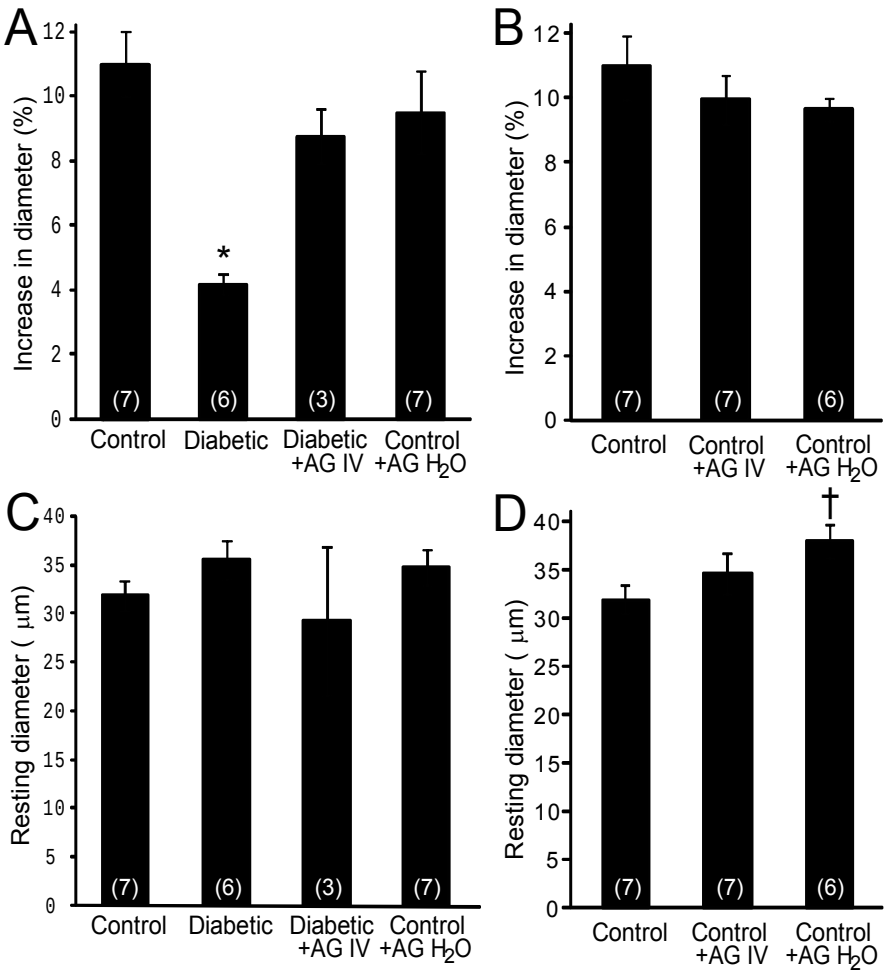

Figure 3. AG treatment reversed the loss of flicker-induced arteriole dilation in diabetic animals. (A) The reduction in flicker-induced vasodilation in diabetic animals was restored by treatment with AG (either IV or in H_2O). (B) AG did not alter flicker-induced vasodilations in control animals. (C) The resting arteriole diameter was similar in all experimental groups. (D) AG treatment slightly increased the resting arteriole diameter in control animals when administered in drinking water, but not when given IV. Numbers in parenthesis indicate number of animals. * indicates $P < 0.0001$, † indicates $P < 0.05$.

The loss of neurovascular coupling could also be due to a decrease in light-evoked neuronal activity in diabetic animals, caused either by a loss of neuronal responsiveness or by neuronal death. We evaluated retinal responsiveness by monitoring the b-wave of the ERG, which primarily reflects ON bipolar cell activity. A series of ERGs were recorded to light flashes of increasing intensities (Fig. 4A). There was no difference in the maximal b-wave amplitude between control and diabetic animals: 0.22 ± 0.01 mV (n = 7) vs. 0.24 ± 0.03 mV (n = 3), respectively ($P > 0.4$; Figs. 4B, 4C). The sensitivity of the retina, evaluated by the light intensity that evoked a half-maximal b-wave response, was also similar: 0.012 ± 0.003 in controls vs. 0.014 ± 0.007 in diabetic rats ($P > 0.7$, where a value of 1 corresponds to 0 log unit intensity; Figs. 4B, 4D). These results indicate that neuronal activity was not reduced in the retinas of our diabetic rats.

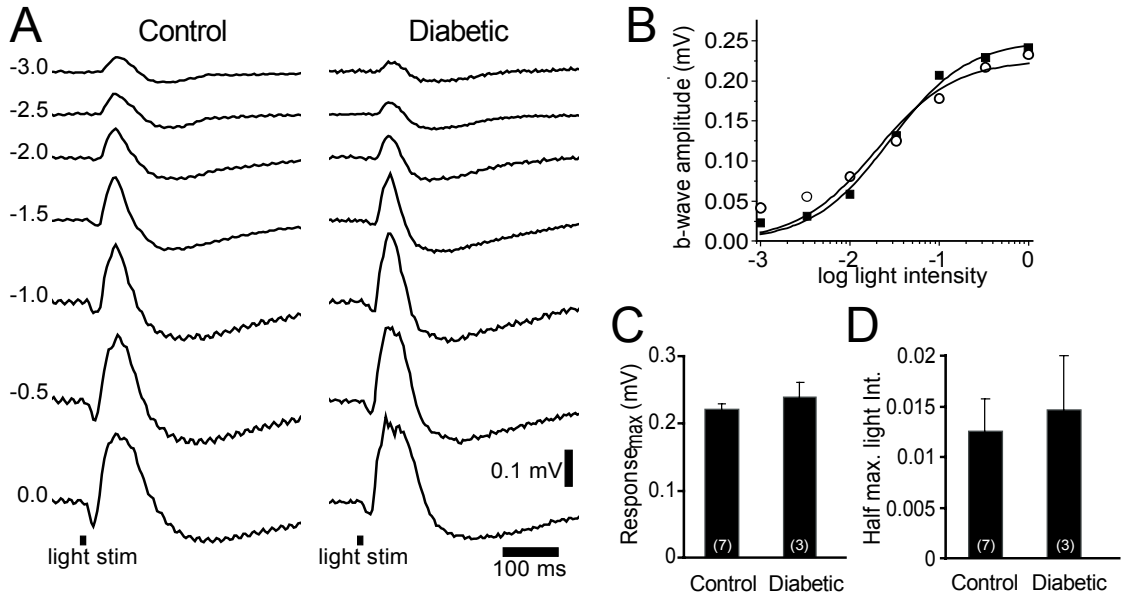

Figure 4. Electroretinogram recordings from control and diabetic animals were similar. (A) Intensity series of ERG traces from a control and a diabetic animal to 10 ms light flashes (black bars at bottom) of increasing intensities (numbers indicate intensity in log units). (B) Intensity-response relations for the control (open circles) and diabetic (black squares) series shown in A. (C-D): The maximum b-wave response (C) and the light intensity evoking a half-maximal b-wave response (D) were similar in control and diabetic animals ($P > 0.4$). The data were fit with the Rushton-Naka relation (125).

Discussion

Our results demonstrate that the iNOS inhibitor AG, delivered either IV or in drinking water, reverses the loss of flicker-induced vasodilation in an animal model of type 1 diabetes. Although AG also inhibits the formation of AGEs, the acute and immediate reversal of light-evoked dilations following IV administration in our experiments suggests that AG is acting by inhibiting iNOS. This view is supported by our observations in the isolated diabetic retina (121), where the specific iNOS inhibitor 1400W also reversed the loss of flicker-induced dilations.

It is unlikely that the loss of flicker-induced dilation is due to a decrease in light-evoked neuronal activity, as the ERG b-wave amplitude and sensitivity were normal in our diabetic animals. In addition, we have shown previously that there is no loss of retinal neurons in our diabetic animals at a 7 month survival time (121).

Several previous animal studies have demonstrated a loss of both retinal neurons and the ERG in early stages of diabetic retinopathy (74;76;120;126). However, most of these studies were conducted using albino strains whose retinas are susceptible to light damage, compounding the effects of diabetic retinopathy. Our experiments are conducted in pigmented Long-Evans rats, a strain that displays a much lower retinal inflammatory response up to four months after induction of diabetes by streptozotocin, compared to changes observed in albino Sprague-Dawley retinas (113). In addition, streptozotocin-treated pigmented mice display an early transient increase in apoptosis, but then show no significant changes in neuronal death up to a year after diabetes induction (110). Collectively, we attribute the absence of neuronal death and the normal ERG response in our diabetic Long-Evans rats to the reduced vulnerability of pigmented eyes to light-damage.

The reduced flicker-induced vasodilation we observed does not appear to be due to a loss of vascular responsiveness. Using the *ex vivo* retina preparation, we demonstrated that prostaglandin E_2-induced dilation of retinal arterioles remains intact in these diabetic animals (121). Additionally, a recent study showed that vascular reactivity to exogenous NO stimulation is unchanged in diabetic patients (73). The rapid reversal of light-induced vasodilation after AG IV treatment also argues against a loss of vascular responsiveness.

Altered signaling from glial cells to blood vessels is the likely cause of reduced flicker-induced vasodilation in diabetic retinas. Flicker-induced vasodilation in the retina is largely mediated by the release of vasodilatory agents from glial cells following neuronal activation (55). Nitric oxide (NO) modulates this signaling pathway by an as-yet unidentified mechanism. Both light and glial stimulation evoke retinal vasodilation when NO levels are low. However, vasodilation is reduced and vasoconstriction enhanced when NO levels are raised (55). Several laboratories have shown an increase in iNOS expression in the diabetic retina (84;121), leading to high NO levels (112). This increase in NO likely inhibits glial release of dilatory agents, disrupting the tight coupling between neuronal activity and vasodilation. It is likely that AG is acting by inhibiting iNOS and lowering retinal NO levels, thus allowing normal signaling to occur between glial cells and the vasculature. Our finding that AG does not alter neurovascular coupling in control animals supports this view, as iNOS expression is minimal in the healthy retina. It is of interest that the onset of reactive gliosis in our diabetic animals coincides with the loss of neurovascular coupling, at a 7 month survival time (121). This is not surprising, as iNOS upregulation is expected to be associated with glial reactivity.

Neurovascular coupling is essential for meeting the increased demand of active retinal neurons for oxygen and glucose (3;80). A disruption of this coupling may induce damage

due to the resulting hypoxia, hypoglycemia, or accumulation of harmful metabolites. Thus, the reduction in flicker-induced vasodilation observed in diabetic patients before the onset of clinical retinopathy could be a contributing factor leading to the development of neuronal and vascular pathology.

AG has been previously investigated as a treatment for complications of diabetes in both animal models and in diabetic patients (112;123;124). Clinical studies have demonstrated the beneficial effects of AG on retinopathy, where significantly fewer patients showed progression of retinopathy (defined as a 3 step or more increase in the Early Treatment Diabetic Retinopathy Study scale) when treated with AG, compared to placebo-treated patients (124). A few adverse effects were observed in some patients, although they only occurred when high AG doses were administered. It is noteworthy that these studies were conducted in patients with existing retinopathy. We suggest that restoration of neurovascular coupling early in the course of diabetes, before the development of visible clinical symptoms, may be more effective in slowing the progression of retinal pathology. Targeting iNOS or its downstream signaling pathway with selective inhibitors to reverse the loss of neurovascular coupling may serve as an effective primary intervention for diabetic retinopathy.

Acknowledgements. The authors thank Elizabeth R. Seaquist (University of Minnesota) and Tess Kornfield (University of Minnesota) for comments on the manuscript, and Michael Burian (University of Minnesota) for expert technical assistance.

Reference List

1. Magistretti PJ, Pellerin L, Martin JL: Brain Energy Metabolism: An Integrated Cellular Perspective. In *Psychopharmacology - 4th Generation of Progress*. 2000,

2. Cipolla MJ: The Cerebral Circulation. In *Integrated Systems Physiology: From Molecule to Function*. Granger DN, Granger JP, Eds. San Rafael, CA, Morgan & Claypool Life Sciences, 2009,

3. Riva,CE, Logean,E, Falsini,B: Visually evoked hemodynamical response and assessment of neurovascular coupling in the optic nerve and retina. *Prog Ret Eye Res* 24:183-215, 2005

4. Delaey,C, Van De Voorde,J: Regulatory mechanisms in the retinal and choroidal circulation. *Ophthalmic Res* 32:249-256, 2000

5. Attwell,D, Buchan,AM, Charpak,S, Lauritzen,M, MacVicar,BA, Newman,EA: Glial and neuronal control of brain blood flow. *Nature* 468:232-243, 2010

6. Rudzinski,W, Swiat,M, Tomaszewski,M, Krejza,J: Cerebral hemodynamics and investigations of cerebral blood flow regulation. *Nucl Med Rev Cent East Eur* 10:29-42, 2007

7. Kontos,HA, Wei,EP: Oxygen-dependent mechanisms in cerebral autoregulation. *Ann Biomed Eng* 13:329-334, 1985

8. Murkin,JM: Cerebral autoregulation: the role of CO2 in metabolic homeostasis. *Semin Cardiothorac Vasc Anesth* 11:269-273, 2007

9. Brian,JE, Jr., Faraci,FM, Heistad,DD: Recent insights into the regulation of cerebral circulation. *Clin Exp Pharmacol Physiol* 23:449-457, 1996

10. Wahl,M, Schilling,L: Regulation of cerebral blood flow- a brief review. *Acta Neurochir* 59:3-10, 1993

11. Pournaras,CJ, Rungger-Brandle,E, Riva,CE, Hardarson,SH, Stefansson,E: Regulation of retinal blood flow in health and disease. *Prog Ret Eye Res* 27:284-330, 2008

12. Mosso,A: Sulla circolazione del sangue nel cervello dell'uomo. *R Accad Lincei* 5:237-358, 1880

13. Roy,CS, Sherrington,CS: On the regulation of the blood-supply of the brain. *J Physiol* 11:85-108, 1890

14. Hamel,E: Perivascular nerves and the regulation of cerebrovascular tone. *J Appl Physiol* 100:1059-1064, 2006

15. Tuor,UI: Acute hypertension and sympathetic stimulation: local heterogeneous changes in cerebral blood flow. *Am J Physiol* 263:H511-H518, 1992

16. Bolay,H, Reuter,U, Dunn,AK, Huang,Z, Boas,DA, Moskowitz,MA: Intrinsic brain activity triggers trigeminal meningeal afferents in a migraine model. *Nat Med* 8:136-142, 2002

17. Zhang,X, Levy,D, Kainz,V, Noseda,R, Jakubowski,M, Burstein,R: Activation of central trigeminovascular neurons by cortical spreading depression. *Ann Neurol* 69:855-865, 2011

18. Vaucher,E, Hamel,E: Cholinergic basal forebrain neurons project to cortical microvessels in the rat: electron microscopic study with anterogradely transported Phaseolus vulgaris leucoagglutinin and choline acetyltransferase immunocytochemistry. *J Neurosci* 15:7427-7441, 1995

19. Hamel,E: Cholinergic modulation of the cortical microvascular bed. *Prog Brain Res* 145:171-178, 2004

20. Cohen,Z, Molinatti,G, Hamel,E: Astroglial and vascular interactions of noradrenaline terminals in the rat cerebral cortex. *J Cereb Blood Flow Metab* 17:894-904, 1997

21. Cohen,Z, Bonvento,G, Lacombe,P, Hamel,E: Serotonin in the regulation of brain microcirculation. *Prog Neurobiol* 50:335-362, 1996

22. Mulligan,SJ, MacVicar,BA: Calcium transients in astrocyte endfeet cause cerebrovascular constrictions. *Nature* 431:195-199, 2004

23. Vaucher,E, Tong,XK, Cholet,N, Lantin,S, Hamel,E: GABA neurons provide a rich input to microvessels but not nitric oxide neurons in the rat cerebral cortex: a means for direct regulation of local cerebral blood flow. *J Comp Neurol* 421:161-171, 2000

24. Cauli,B, Tong,XK, Rancillac,A, Serluca,N, Lambolez,B, Rossier,J, Hamel,E: Cortical GABA interneurons in neurovascular coupling: relays for subcortical vasoactive pathways. *J Neurosci* 24:8940-8949, 2004

25. Ventura,R, Harris,KM: Three-dimensional relationships between hippocampal synapses and astrocytes. *J Neurosci* 19:6897-6906, 1999

26. Bushong,EA, Martone,ME, Jones,YZ, Ellisman,MH: Protoplasmic astrocytes in CA1 stratum radiatum occupy separate anatomical domains. *J Neurosci* 22:183-192, 2002

27. Haber,M, Zhou,L, Murai,KK: Cooperative astrocyte and dendritic spine dynamics at hippocampal excitatory synapses. *J Neurosci* 26:8881-8891, 2006

28. Porter,JT, McCarthy,KD: Hippocampal astrocytes *in situ* respond to glutamate released from synaptic terminals. *J Neurosci* 16:5073-5081, 1996

29. Piet,R, Jahr,CE: Glutamatergic and purinergic receptor-mediated calcium transients in Bergmann glial cells. *J Neurosci* 27:4027-4035, 2007

30. Newman,EA: Calcium increases in retinal glial cells evoked by light-induced neuronal activity. *J Neurosci* 25:5502-5510, 2005

31. Schipke,CG, Kettenmann,H: Astrocyte responses to neuronal activity. *Glia* 47:226-232, 2004

32. Simard,M, Arcuino,G, Takano,T, Liu,QS, Nedergaard,M: Signaling at the gliovascular interface. *J Neurosci* 23:9254-9262, 2003

33. Paulson,OB, Newman,EA: Does the release of potassium from astrocyte endfeet regulate cerebral blood flow? *Science* 237:896-898, 1987

34. Karwoski,CJ, Proenza,LM: Light-evoked changes in extracellular potassium concentration in mudpuppy retina. *Brain Res* 142:515-530, 1978

35. Karwoski,CJ, Newman,EA, Shimazaki,H, Proenza,LM: Light-evoked increases in extracellular K^+ in the plexiform layers of amphibian retinas. *J Gen Physiol* 86:189-213, 1985

36. Karwoski,CJ, Lu,HK, Newman,EA: Spatial buffering of light-evoked potassium increases by retinal Muller (glial) cells. *Science* 244:578-580, 1989

37. Newman,EA: Inward-rectifying potassium channels in retinal glial (Muller) cells. *J Neurosci* 13:3333-3345, 1993

38. Knot,HJ, Zimmererman,PA, Nelson,MT: Extracellular K^+-induced hyperpolarizations and dilatations of rat coronary and cerebral arteries involve inward rectifier K^+ channels. *J Physiol* 492.2:419-430, 1996

39. Metea,MR, Kofuji,P, Newman,EA: Neurovascular coupling is not mediated by potassium siphoning from glial cells. *J Neurosci* 27:2468-2471, 2007

40. Filosa,JA, Bonev,AD, Straub,SV, Meredith,AL, Wilkerson,MK, Aldrich,RW, Nelson,MT: Local potassium signaling couples neuronal activity to vasodilation in the brain. *Nat Neurosci* 9:1397-1403, 2006

41. Amruthesh,SC, Boerschel,MF, McKinney,JS, Willoughby,KA, Ellis,EF: Metabolism of arachidonic acid to epoxyeicosatrienoic acids, hydroxyeicosatetraenoic acids, and prostaglandins in cultured rat hippocampal astrocytes. *J Neurochem* 61:150-159, 1993

42. Alkayed,NJ, Narayanan,J, Gebremedhin,D, Medhora,M, Roman,RJ, Harder,DR: Molecular characterization of an arachidonic acid epoxygenase in rat brain astrocytes. *Stroke* 27:971-979, 1996

43. Gebremedhin,D, Lange,AR, Lowry,TF, Taheri,MR, Birks,EK, Hudetz,AG, Narayanan,J, Falck,JR, Okamoto,H, Roman,RJ, Nithipatikom,K, Campbell,WB,

Harder,DR: Production of 20-HETE and its role in autoregulation of cerebral blood flow. *Circ Res* 87:60-65, 2000

44. Roman,RJ: P-450 metabolites of arachidonic acid in the control of cardiovascular function. *Physiol Rev* 82:131-185, 2002

45. Jackson,WF: Potassium channels in the peripheral microcirculation. *Microcirculation* 12:113-127, 2005

46. Behm,DJ, Ogbonna,A, Wu,C, Burns-Kurtis,CL, Douglas,SA: Epoxyeicosatrienoic acids function as selective, endogenous antagonists of native thromboxane receptors: identification of a novel mechanism of vasodilation. *J Pharmacol Exp Ther* 328:231-239, 2009

47. Abran,D, Dumont,I, Hardy,P, Peri,K, Li,DY, Molotchnikoff,S, Varma,DR, Chemtob,S: Characterization and regulation of prostaglandin E2 receptor and receptor-coupled functions in the choroidal vasculature of the pig during development. *Circ Res* 80:463-472, 1997

48. Davis,RJ, Murdoch,CE, Ali,M, Purbrick,S, Ravid,R, Baxter,GS, Tilford,N, Sheldrick,RL, Clark,KL, Coleman,RA: EP4 prostanoid receptor-mediated vasodilatation of human middle cerebral arteries. *Br J Pharmacol* 141:580-585, 2004

49. Jadhav,V, Jabre,A, Lin,SZ, Lee,TJ: EP1- and EP3-receptors mediate prostaglandin E2-induced constriction of porcine large cerebral arteries. *J Cereb Blood Flow Metab* 24:1305-1316, 2004

50. Harder,DR, Alkayed,NJ, Lange,AR, Gebremedhin,D, Roman,RJ: Functional hyperemia in the brain: hypothesis for astrocyte-derived vasodilator metabolites. *Stroke* 29:229-234, 1998

51. Peng,X, Carhuapoma,JR, Bhardwaj,A, Alkayed,NJ, Falck,JR, Harder,DR, Traystman,RJ, Koehler,RC: Suppression of cortical functional hyperemia to vibrissal stimulation in the rat by epoxygenase inhibitors. *Am J Physiol Heart Circ Physiol* 283:H2029-H2037, 2002

52. Zonta,M, Angulo,MC, Gobbo,S, Rosengarten,B, Hossmann,KA, Pozzan,T, Carmignoto,G: Neuron-to-astrocyte signaling is central to the dynamic control of brain microcirculation. *Nat Neurosci* 6:43-50, 2003

53. Takano,T, Tian,GF, Peng,W, Lou,N, Libionka,W, Han,X, Nedergaard,M: Astrocyte-mediated control of cerebral blood flow. *Nat Neurosci* 9:260-267, 2006

54. Patton,N, Aslam,T, Macgillivray,T, Pattie,A, Deary,IJ, Dhillon,B: Retinal vascular image analysis as a potential screening tool for cerebrovascular disease: a rationale based on homology between cerebral and retinal microvasculatures. *J Anat* 206:319-348, 2005

55. Metea,MR, Newman,EA: Glial cells dilate and constrict blood vessels: a mechanism of neurovascular coupling. *J Neurosci* 26:2862-2870, 2006

56. Palmer,RM, Ferrige,AG, Moncada,S: Nitric oxide release accounts for the biological activity of endothelium-derived relaxing factor. *Nature* 327:524-526, 1987

57. Ignarro,LJ: Nitric oxide as a unique signaling molecule in the vascular system: a historical overview. *J Physiol Pharmacol* 53:t-14, 2002

58. Kessler,P, Popp,R, Busse,R, Schini-Kerth,VB: Proinflammatory mediators chronically downregulate the formation of the endothelium-derived hyperpolarizing factor in arteries via a nitric oxide/cyclic GMP-dependent mechanism. *Circulation* 99:1878-1884, 1999

59. Gordon,GRJ, Choi,HB, Rungta,RL, Ellis-Davies,GCR, MacVicar,BA: Brain metabolism dictates the polarity of astrocyte control over arterioles. *Nature* 456:745-749, 2008

60. Lindauer,U, Leithner,C, Kaasch,H, Rohrer,B, Foddis,M, Fuchtemeier,M, Offenhauser,N, Steinbrink,J, Royl,G, Kohl-Bareis,M, Dirnagl,U: Neurovascular coupling in rat brain operates independent of hemoglobin deoxygenation. *J Cereb Blood Flow Metab* 30:757-768, 2010

61. Kanai,N, Lu,R, Satriano,JA, Bao,Y, Wolkoff,AW, Schuster,VL: Identification and characterization of a prostaglandin transporter. *Science* 268:866-869, 1995

62. Chan,BS, Endo,S, Kanai,N, Schuster,VL: Identification of lactate as a driving force for prostanoid transport by prostaglandin transporter PGT. *Am J Physiol Renal Physiol* 282:F1097-F1102, 2002

63. Abu-Soud,HM, Rousseau,DL, Stuehr,DJ: Nitric oxide binding to the heme of neuronal nitric-oxide synthase links its activity to changes in oxygen tension. *J Biol Chem* 271:32515-32518, 1996

64. Stuehr,DJ, Santolini,J, Wang,ZQ, Wei,CC, Adak,S: Update on mechanism and catalytic regulation in the NO synthases. *J Biol Chem* 279:36167-36170, 2004

65. Harder,DR, Narayanan,J, Birks,EK, Liard,JF, Imig,JD, Lombard,JH, Lange,AR, Roman,RJ: Identification of a putative microvascular oxygen sensor. *Circ Res* 79:54-61, 1996

66. Juránek,I, Suzuki,H, Yamamoto,S: Affinities of various mammalian arachidonate lipoxygenases and cyclooxygenases for molecular oxygen as substrate. *Biochim Biophys Acta* 1436:509-518, 1999

67. Nagel,E, Vilser,W, Lanzl,I: Age, blood pressure, and vessel diameter as factors influencing the arterial retinal flicker response. *Invest Ophthalmol Vis Sci* 45:1486-1492, 2004

68. Garhofer,G, Zawinka,C, Resch,H, Huemer,KH, Schmetterer,L, Dorner,GT: Response of retinal vessel diameters to flicker stimulation in patients with early open angle glaucoma. *J Glaucoma* 13:340-344, 2004

69. Riva,CE, Salgarello,T, Logean,E, Colotto,A, Galan,EM, Falsini,B: Flicker-evoked response measured at the optic disc rim is reduced in ocular hypertension and early glaucoma. *Invest Ophthalmol Vis Sci* 45:3662-3668, 2004

70. Garhofer,G, Zawinka,C, Resch,H, Kothy,P, Schmetterer,L, Dorner,GT: Reduced response of retinal vessel diameters to flicker stimulation in patients with diabetes. *Br J Ophthalmol* 88:887-891, 2004

71. Mandecka,A, Dawczynski,J, Blum,M, Muller,N, Kloos,C, Wolf,G, Vilser,W, Hoyer,H, Muller,UA: Influence of flickering light on the retinal vessels in diabetic patients. *Diabetes Care* 30:3048-3052, 2007

72. Nguyen,TT, Kawasaki,R, Wang,JJ, Kreis,AJ, Shaw,J, Vilser,W, Wong,TY: Flicker light-induced retinal vasodilation in diabetes and diabetic retinopathy. *Diabetes Care* 32:2075-2080, 2009

73. Pemp,B, Garhofer,G, Weigert,G, Karl,K, Resch,H, Wolzt,M, Schmetterer,L: Reduced retinal vessel response to flicker stimulation but not to exogenous nitric oxide in type 1 diabetes. *Invest Ophthalmol Vis Sci* 50:4029-4032, 2009

74. Antonetti,DA, Barber,AJ, Bronson,SK, Freeman,WM, Gardner,TW, Jefferson,LS, Kester,M, Kimball,SR, Krady,JK, LaNoue,KF, Norbury,CC, Quinn,PG, Sandirasegarane,L, Simpson,IA: Diabetic retinopathy: seeing beyond glucose-induced microvascular disease. *Diabetes* 55:2401-2411, 2006

75. Mizutani,M, Kern,TS, Lorenzi,M: Accelerated death of retinal microvascular cells in human and experimental diabetic retinopathy. *J Clin Invest* 97:2883-2890, 1996

76. Barber,AJ, Lieth,E, Khin,SA, Antonetti,DA, Buchanan,AG, Gardner,TW: Neural apoptosis in the retina during experimental and human diabetes. Early onset and effect of insulin. *J Clin Invest* 102:783-791, 1998

77. Hancock,HA, Kraft,TW: Oscillatory potential analysis and ERGs of normal and diabetic rats. *Invest Ophthalmol Vis Sci* 45:1002-1008, 2004

78. Lieth,E, Barber,AJ, Xu,B, Dice,C, Ratz,MJ, Tanase,D, Strother,JM: Glial reactivity and impaired glutamate metabolism in short-term experimental diabetic retinopathy. *Diabetes* 47:815-820, 1998

79. Mizutani,M, Gerhardinger,C, Lorenzi,M: Müller cell changes in human diabetic retinopathy. *Diabetes* 47:445-449, 1998

80. Polak,K, Schmetterer,L, Riva,CE: Influence of flicker frequency on flicker-induced changes of retinal vessel diameter. *Invest Ophthalmol Vis Sci* 43:2721-2726, 2002

81. Abu El-Asrar,AM, Desmet,S, Meersschaert,A, Dralands,L, Missotten,L, Geboes,K: Expression of the inducible isoform of nitric oxide synthase in the retinas of human subjects with diabetes mellitus. *Am J Ophthalmol* 132:551-556, 2001

82. Du,Y, Sarthy,VP, Kern,TS: Interaction between NO and COX pathways in retinal cells exposed to elevated glucose and retina of diabetic rats. *Am J Physiol Regul Integr Comp Physiol* 287:R735-R741, 2004

83. Toda,N, Nakanishi-Toda,M: Nitric oxide: ocular blood flow, glaucoma, and diabetic retinopathy. *Prog Ret Eye Res* 26:205-238, 2007

84. Du,Y, Smith,MA, Miller,CM, Kern,TS: Diabetes-induced nitrative stress in the retina, and correction by aminoguanidine. *J Neurochem* 80:771-779, 2002

85. Alkayed,NJ, Birks,EK, Narayanan,J, Petrie,KA, Kohler-Cabot,AE, Harder,DR: Role of P-450 arachidonic acid epoxygenase in the response of cerebral blood flow to glutamate in rats. *Stroke* 28:1066-1072, 1997

86. Liu,X, Li,C, Gebremedhin,D, Hwang,SH, Hammock,BD, Falck,JR, Roman,RJ, Harder,DR, Koehler,RC: Epoxyeicosatrienoic acid-dependent cerebral vasodilation evoked by metabotropic glutamate receptor activation in vivo. *Am J Physiol Heart Circ Physiol* 2011

87. Yu,DY, Cringle,SJ, Alder,VA, Su,EN: Intraretinal oxygen distribution in rats as a function of systemic blood pressure. *Am J Physiol* 267:H2498-H2507, 1994

88. Yu,DY, Cringle,SJ, Alder,V, Su,EN: Intraretinal oxygen distribution in the rat with graded systemic hyperoxia and hypercapnia. *Invest Ophthalmol Vis Sci* 40:2082-2087, 1999

89. Zonta,M, Sebelin,A, Gobbo,S, Fellin,T, Pozzan,T, Carmignoto,G: Glutamate-mediated cytosolic calcium oscillations regulate a pulsatile prostaglandin release from cultured rat astrocytes. *J Physiol* 553:407-414, 2003

90. Metzger,H, Erdmann,W, Thews,G: Effect of short periods of hypoxia, hyperoxia, and hypercapnia on brain O 2 supply. *J Appl Physiol* 31:751-759, 1971

91. Zhang,J, Sam,AD, Klitzman,B, Piantadosi,CA: Inhibition of nitric oxide synthase on brain oxygenation in anesthetized rats exposed to hyperbaric oxygen. *Undersea Hyperb Med* 22:377-382, 1995

92. O'Hara,JA, Hou,H, Demidenko,E, Springett,RJ, Khan,N, Swartz,HM: Simultaneous measurement of rat brain cortex PtO_2 using EPR oximetry and a fluorescence fiber-optic sensor during normoxia and hyperoxia. *Physiol Meas* 26:203-213, 2005

93. Hickam,JB, Frayser,R: Studies of the retinal circulation in man: observations on vessel diameter, arteriovenous oxygen difference, and mean circulation time. *Circulation* 33:302-316, 1966

94. Eperon,G, Johnson,M, David,NJ: The effect of arterial PO2 on relative retinal blood flow in monkeys. *Invest Ophthalmol* 14:342-352, 1975

95. Stogner,SW, Payne,DK: Oxygen toxicity. *Ann Pharmacother* 26:1554-1562, 1992

96. Wijayanti,N, Katz,N, Immenschuh,S: Biology of heme in health and disease. *Curr Med Chem* 11:981-986, 2004

97. Elayan,IM, Axley,MJ, Prasad,PV, Ahlers,ST, Auker,CR: Effect of hyperbaric oxygen treatment on nitric oxide and oxygen free radicals in rat brain. *J Neurophysiol* 83:2022-2029, 2000

98. Srienc,AI, Kurth-Nelson,ZL, Newman,EA: Imaging retinal blood flow with laser speckle flowmetry. *Front Neuroenerg* 2:128, 2010

99. Filosa,JA, Bonev,AD, Nelson,MT: Calcium dynamics in cortical astrocytes and arterioles during neurovascular coupling. *Circ Res* 95:e73-e81, 2004

100. Koehler,RC, Roman,RJ, Harder,DR: Astrocytes and the regulation of cerebral blood flow. *Trends Neurosci* 32:160-169, 2009

101. Ellis,EF, Wei,EP, Kontos,HA: Vasodilation of cat cerebral arterioles by prostaglandins D2, E2, G2, and I2. *Am J Physiol* 237:H381-H385, 1979

102. Amruthesh,SC, Falck,JR, Ellis,EF: Brain synthesis and cerebrovascular action of epoxygenase metabolites of arachidonic acid. *J Neurochem* 58:503-510, 1992

103. Harder,DR, Gebremedhin,D, Narayanan,J, Jefcoat,C, Falck,JR, Campbell,WB, Roman,R: Formation and action of a P-450 4A metabolite of arachidonic acid in cat cerebral microvessels. *Am J Physiol* 266:H2098-H2107, 1994

104. Yu,DY, Cringle,SJ, Su,EN, Yu,PK, Jerums,G, Cooper,ME: Pathogenesis and intervention strategies in diabetic retinopathy. *Clin Experiment Ophthalmol* 29:164-166, 2001

105. Rungger-Brandle,E, Dosso,AA: Streptozotocin-induced diabetes--a rat model to study involvement of retinal cell types in the onset of diabetic retinopathy. *Adv Exp Med Biol* 533:197-203, 2003

106. Newman,EA: Propagation of intercellular calcium waves in retinal astrocytes and Müller cells. *J Neurosci* 21:2215-2223, 2001

107. Blanco,VM, Stern,JE, Filosa,JA: Tone-dependent vascular responses to astrocyte-derived signals. *Am J Physiol Heart Circ Physiol* 294:H2855-H2863, 2008

108. Mishra,A, Srienc,AI, Clark,BD, Newman,EA: Oxygen modulates functional hyperemia in the retina. *Soc Neurosci Abstr* In press: 2010

109. van Dijk,HW, Kok,PH, Garvin,M, Sonka,M, Devries,JH, Michels,RP, van Velthoven,ME, Schlingemann,RO, Verbraak,FD, Abramoff,MD: Selective loss of inner retinal layer thickness in type 1 diabetic patients with minimal diabetic retinopathy. *Invest Ophthalmol Vis Sci* 50:3404-3409, 2009

110. Feit-Leichman,RA, Kinouchi,R, Takeda,M, Fan,Z, Mohr,S, Kern,TS, Chen,DF: Vascular damage in a mouse model of diabetic retinopathy: relation to neuronal and glial changes. *Invest Ophthalmol Vis Sci* 46:4281-4287, 2005

111. Li,Q, Puro,DG: Diabetes-induced dysfunction of the glutamate transporter in retinal Müller cells. *Invest Ophthalmol Vis Sci* 43:3109-3116, 2002

112. Kowluru,RA, Engerman,RL, Kern,TS: Abnormalities of retinal metabolism in diabetes or experimental galactosemia VIII. Prevention by aminoguanidine. *Curr Eye Res* 21:814-819, 2000

113. Kirwin,SJ, Kanaly,ST, Linke,NA, Edelman,JL: Strain-dependent increases in retinal inflammatory proteins and photoreceptor FGF-2 expression in streptozotocin-induced diabetic rats. *Invest Ophthalmol Vis Sci* 50:5396-5404, 2009

114. Cattell,V, Jansen,A: Inducible nitric oxide synthase in inflammation. *Histochem J* 27:777-784, 1995

115. Alder,VA, Su,EN, Yu,DY, Cringle,SJ, Yu,PK: Diabetic retinopathy: early functional changes. *Clin Exp Pharmacol Physiol* 24:785-788, 1997

116. Gariano,RF, Gardner,TW: Retinal angiogenesis in development and disease. *Nature* 438:960-966, 2005

117. Brownlee,M, Vlassara,H, Kooney,A, Ulrich,P, Cerami,A: Aminoguanidine prevents diabetes-induced arterial wall protein cross-linking. *Science* 232:1629-1632, 1986

118. Hammes,HP, Martin,S, Federlin,K, Geisen,K, Brownlee,M: Aminoguanidine treatment inhibits the development of experimental diabetic retinopathy. *Proc Natl Acad Sci U S A* 88:11555-11558, 1991

119. Corbett,JA, Tilton,RG, Chang,K, Hasan,KS, Ido,Y, Wang,JL, Sweetland,MA, Lancaster,JR, Jr., Williamson,JR, McDaniel,ML: Aminoguanidine, a novel inhibitor of nitric oxide formation, prevents diabetic vascular dysfunction. *Diabetes* 41:552-556, 1992

120. Fletcher,EL, Phipps,JA, Ward,MM, Puthussery,T, Wilkinson-Berka,JL: Neuronal and glial cell abnormality as predictors of progression of diabetic retinopathy. *Curr Pharm Des* 13:2699-2712, 2007

121. Mishra,A, Newman,EA: Inhibition of inducible nitric oxide synthase reverses the loss of functional hyperemia in diabetic retinopathy. *Glia* 58:1996-2004, 2010

122. Griffiths,MJ, Messent,M, MacAllister,RJ, Evans,TW: Aminoguanidine selectively inhibits inducible nitric oxide synthase. *Br J Pharmacol* 110:963-968, 1993

123. Kern,TS, Engerman,RL: Pharmacological inhibition of diabetic retinopathy: aminoguanidine and aspirin. *Diabetes* 50:1636-1642, 2001

124. Bolton,WK, Cattran,DC, Williams,ME, Adler,SG, Appel,GB, Cartwright,K, Foiles,PG, Freedman,BI, Raskin,P, Ratner,RE, Spinowitz,BS, Whittier,FC, Wuerth,JP, ACTION,I, I: Randomized trial of an inhibitor of formation of advanced glycation end products in diabetic nephropathy. *Am J Nephrol* 24:32-40, 2004

125. Naka,KI, Rushton,WA: S-potentials from luminosity units in the retina of fish (Cyprinidae). *J Physiol* 185:587-599, 1966

126. Phipps,JA, Fletcher,EL, Vingrys,AJ: Paired-flash identification of rod and cone dysfunction in the diabetic rat. *Invest Ophthalmol Vis Sci* 45:4592-4600, 2004